

Received September 10, 2019, accepted October 17, 2019, date of publication November 1, 2019,
date of current version November 18, 2019.

Digital Object Identifier 10.1109/ACCESS.2019.2950911

Power Quality Issues of Distorted and Weak Distribution Networks in Mining Industry: A Review

JALIL YAGHOobi¹, (Member, IEEE), AHMAD ABDULLAH¹,
DINESH KUMAR², (Member, IEEE), FIRUZ ZARE¹, (Senior Member, IEEE),
AND HAMID SOLTANI³, (Member, IEEE)

¹School of Information Technology and Electrical Engineering, The University of Queensland, Brisbane, QLD 4067, Australia

²Global Research and Development Center, Danfoss Drives A/S, 6300 Gråsten, Denmark

³Vestas Wind Systems A/S, 8000 Aarhus, Denmark

Corresponding author: Jalil Yaghoobi (j.yaghoobi@uq.edu.au)

This work was supported by the Australian Research Council under Project FT150100042, Project LP170100902, and Project LP160101675.

ABSTRACT Mining is an important industry in many countries including Australia and plays a vital role in their economy. The industry heavily depends on electricity as it employs different types of electrical loads. Consequently, a stable and reliable supply of electricity is vital for running the production smoothly. In this review paper, electrical characteristics of mining power systems are described and common power quality and energy efficiency concerns in these systems are stated and classified. Different types of common power electronics topologies used in the industry are also studied and main requirements for reliable and robust operation of the system are categorized. A comprehensive case study to elaborate power quality challenges in mining distribution network is performed.

INDEX TERMS Distorted grid, distribution network, energy efficiency, mining industry, power quality, power system robustness.

I. INTRODUCTION

Mining has been an occupation of mankind since pre-historic times. It has been used for obtaining metals to make required tools for agricultural activities [1]. Mining has been one of the main pillars of the Australian economy for more than 200 years [2]. During the year 2016-2017, the mining sector grew by 1.8% [3]. In 2017, the mining exports of the country increased by 33.8% to \$156.4 billion as compared to the previous year due to higher prices and mining sector recorded the highest increase in operating profits. Although the investments has recently declined, it is still the most significant export part, contributing 5.8% towards the Australian GDP during 2016-2017 [4]. Mining can be classified into three categories depending on the excavation techniques: underground mining including room and pillar, and longwall types, surface mining including open-pit and strip types, and offshore mining. According to [2], the presence of coal in Australia was confirmed in Port Jackson, Sydney in 1791 and the actual mining activities started in 1801 in Hunter Valley,

New South Wales. Authors in [5] have discussed the evolution of mining industry when electricity was introduced in the US underground coal mines at the end of the 19th century. Steam engine driven generators produced DC voltage of 300 V for power distribution to energize series wound DC motors due to their favorable torque-speed characteristics. Coal cutting, drilling, and loading machines were developed at first followed by shuttle car, roof bolting systems, and continuous mining machines. The mechanization resulted in tremendous efficiency enhancement of the mining process; however, it also introduced hazards like electric spark, resulting in safety-related challenges during that era. Even though some mines used a higher voltage of 600 V_{dc}, large voltage drop due to the higher current in DC distribution systems was the root cause for their demise in the 1960s. Consequently, as mentioned in [6], AC distribution systems were introduced in the mining industry during the 1960s with distribution voltage levels up to 4160 V (utilization voltage up to 460 V) by employing various protection schemes.

In this paper, sections 2, 3, and 4 discuss different electrical characteristics of mining plants like power distribution and generation systems, load types, power electronic systems and

The associate editor coordinating the review of this manuscript and approving it for publication was Negareh Ghasemi¹.

their different topologies, energy efficiency, electric trucks, and renewable energy integration. Section 5 investigates different power quality issues in the mining industry along with the mitigation techniques, whereas section 6 focuses on the effect of power quality issues on the reliability and robustness of industrial grids. A comprehensive power quality case study is carried out in Section 7. Conclusions and recommendations are finally presented in Section 8.

II. ELECTRICAL CHARACTERISTICS OF MINING POWER SYSTEMS

The electrical power systems of mining sector are complex due to addition of non-linear loads and higher power requirements. Consequently, different voltage levels and power distribution systems are used in the industry depending on the type of mining. Australian standard AS/NZS 4871.1:2012 [7] defines three voltage levels for mines and quarries power systems: extra low voltage (less than 50 V_{ac} or 120 V_{dc}), low voltage (between 50-1000 V_{ac} or 120-1500 V_{dc}), and high voltage (exceeding low voltage). Similarly, several safety rules and regulations have been created by the Mining Enforcement Safety Administration (MESA) and following voltage levels have been defined for AC as per federal regulations for coal mines in the USA [6]: low voltage (less than 660 V), medium voltage (660-1000 V), and high voltage (higher than 1000 V). Due to the increase in power requirement, the distribution voltage levels have now reached up to 25 kV_{ac}. AC shuttle cars have replaced DC shuttle cars and AC motors with power electronic systems have replaced DC transition motors. Utilization voltages of shuttle cars and continuous miners have also increased to 550 V_{ac} and 2400 V_{ac} respectively. Electric power distribution systems for mines can be classified into three categories depending on the type of excavation technique including underground, surface, and deep-sea mining systems. Power transmission and distribution systems above the earth surface are quite similar for all types of mining systems, but, complexities and differences arise when power is distributed underground or in offshore mines. Power can be supplied to the mining industry from either utility companies or self-power generation using fossil fuels and renewable energy sources.

As mentioned in [8], the power requirement for mining and concentrator plants can be up to 120 MW for 100,000 tons of mining product per day. Nowadays, higher short-circuit capacity is required due to the usage of non-linear loads. This higher short-circuit capacity can be achieved by: (a) adding overhead transmission lines in parallel, (b) increasing the voltage level, (c) using DC transmission, or (d) generating power at the plant. Power generation at the plant site improves the weak grid characteristics, but transportation of fuel and other logistic problems might outweigh the advantages. Nevertheless, mining industries usually use self-generation at remote locations [8]–[10]. The generators are normally driven by diesel engines or fossil fuel-fired boilers. Moreover, emergency diesel generators are extensively used to provide power to critical loads such as hoists, lube oil pumps, and ventilation

fans in case of blackouts. However, as generators cannot respond to load variations as quickly as the utility company, systems with generators operating in island mode are more prone to voltage and frequency fluctuations [8].

A. ELECTRIC POWER DISTRIBUTION SYSTEMS IN UNDERGROUND MINING

Distribution voltages for underground longwall systems have increased due to higher size and power of mining machines, and larger inrush currents and voltage drops due to long cables [5]. The initial power rating of 5 kVA for continuous mining applications has increased to 9 MVA for longwall systems. Nowadays, cycloconverters up to 25 MW are used in underground mining [11]. A simplified single line diagram of one such grinding mill power plant consisting of a 13 MW Semi-Autogenous Grinding (SAG) mill and two 7.83 MW ball mills is shown in Fig. 1. In the substation, power is transformed from 230 kV transmission voltage to distribution voltage level of 11 kV through two 40 MVA transformers. It is then transmitted to loads through power distribution substations.

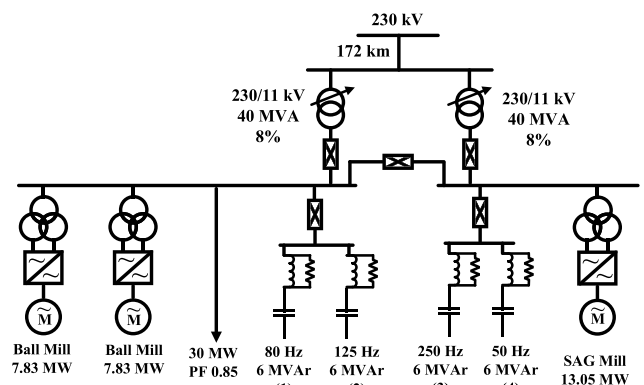


FIGURE 1. Single line diagram of a simplified concentrator plant [12].

As per [8], underground distribution systems for coal are mostly radial due to the mine nature and service requirements, whereas secondary-selective main substations are usually used for improved reliability. The latter consists of a pair of substations connected via a normally open tie-breaker allowing interruption-free maintenance activities of primary circuits. However, radial systems are more economical as compared to the secondary-selective systems.

The underground electrical equipment needs to be portable, durable, and classified for hazardous areas [8]. In this type of environment, maintenance and modifications in the equipment are difficult due to limited space and stringent safety regulations. Authors in [13] have reviewed the grounding issues in underground coal mining industry and the criteria for choosing an appropriate grounding scheme. As the environment is wet and a significant amount of methane gas is present underground, earth faults can lead to a disaster. The inability to detect the first earth fault and the risk of transient overvoltage show that the scheme with no reference to earth

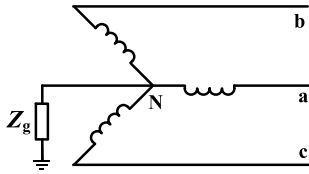


FIGURE 2. A three-phase transformer with high-impedance grounding.

is unsuitable for the mining applications. The low impedance earthing scheme is also impractical due to the high probability of fire and large touch potentials. Hence, high impedance grounding shown in Fig. 2 is the most suitable and widely used scheme in the Australian and worldwide coal mining industries. This grounding method can be used to detect the earth faults and limit the fault energy levels and touch potentials within the range provided by the international standards such as AS/NZS 4871.1 [7] and IEEE Std. 142 [14].

Authors in [15] have mentioned negative impacts of high distribution capacitance as loss of relay selectivity and over-voltage in typical mining industrial systems by referring to the results in [16]–[19]. High impedance grounding scheme has been recommended and it has been proposed to select the value of resistance according to IEEE Std. 142. A detailed design procedure has been presented in [18] and the results have been verified using SPICE simulations for a mine distribution and a high voltage longwall utilization systems.

B. ELECTRIC POWER DISTRIBUTION SYSTEMS IN SURFACE MINING

The equipment for surface mining is mobile and the distribution scheme should consider this mobility [8]. Radial distribution systems are most popular and a section of the primary distribution is established as a baseline consisting of overhead pole lines allowing mobility of the mining equipment [8]. An example of a radial power distribution system of an open pit surface mining industry is given in [20]. This type of system has the advantage of being inexpensive and flexible. Power is transformed in utility substation from transmission voltage of 220 kV to distribution voltage level of 13.8 kV [20].

C. ELECTRIC POWER DISTRIBUTION SYSTEMS IN DEEP-SEA MINING

AC and DC distribution systems have been introduced for deep-sea mining in [21] as shown in Fig. 3. DC system is more economical, efficient, and reliable with reduced cable insulation size and number of components. Hence, they could be a possible future choice if the limitations regarding the lack of galvanic isolation and the incapability of medium voltage circuit breakers to extinguish the short-circuit currents are addressed. The ingress protection (IP) ratings of deep-sea electrical equipment should be selected according to the depth of equipment and required degree of protection.

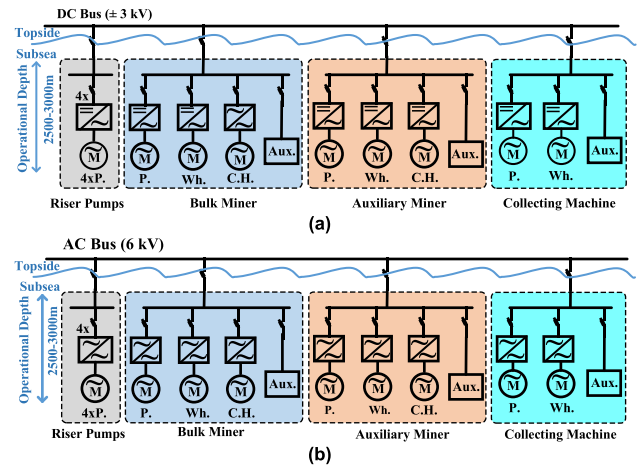


FIGURE 3. Deep-sea mining distribution systems: (a) DC, (b) AC [21].

III. POWER ELECTRONICS TOPOLOGIES

Several types of electrical equipment are used in mining industries. In underground mining, electric locomotives, drills, shearers, crushers, loading machines, belt and shuttle conveyors, roof bolting machines, hoists, chillers, ventilation systems, and different types of pumps are used [5], [6], [8], [22]–[28]. In surface mining, major types of loads include electric draglines, Electric Rope Shovels (ERS), Hydraulic Mining Shovels (HMS), drills, surface bucket-wheel and bucket-chain excavators [8], [10], [20], [29], [30]. The extracted material is transported to mineral processing plants, where crushers, high-pressure grinding rolls, SAG and ball mills, and exhaust and dryer combustion fans are the major load types [8], [11], [31], [32]. Induction and DC motors are used to drive these loads using different AC and DC drives. Since Mercury-arc rectifiers were replaced by the silicon diode in the 1970s [5], the use of power electronic devices in mines has been increasing thanks to technological advancements. According to [8], 80% of the total power in the mining industry is consumed by Adjustable Speed Drives (ASDs). Some of the major power electronic devices include cycloconverters, ASDs, DC-DC converters, rectifiers, active filters, Static Synchronous Compensators (STATCOM), and Static VAR Compensators (SVC) [5], [33]. It is important to analyze how electrical power flows between AC and DC networks. Common AC-DC energy conversion systems are mentioned in the following sections.

A. DIODE AND CONTROLLED RECTIFIERS

Diode and controlled rectifiers are unidirectional power flow topologies and their line currents are distorted by significant low order harmonics, mainly below 2 kHz. There are several solutions to improve the quality of the line current such as passive filters in the DC link and/or in the front side of the rectifier. These rectifiers can be either a single- or a three-phase system as shown in Fig. 4.

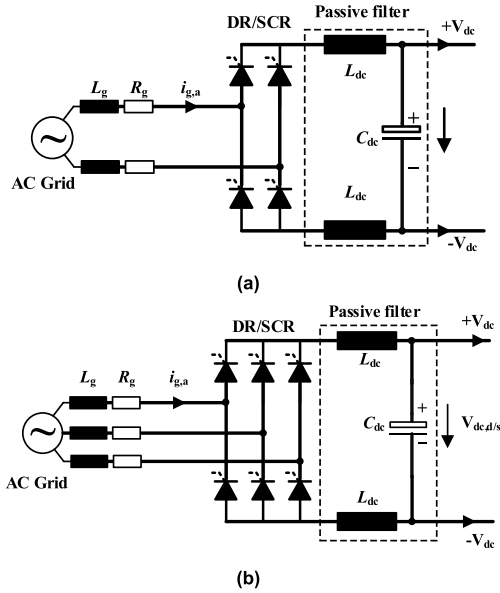


FIGURE 4. Diode or controlled rectifier (a) single-phase, and (b) three-phase.

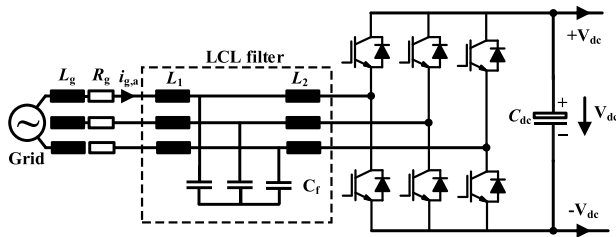


FIGURE 5. AFE with integrated LCL filter.

B. ACTIVE FRONT END (AFE)

This is a bidirectional power flow converter, which provides a high-quality sinusoidal line current waveform. The system has six active power switches such as IGBTs or MOSFETs, controlled based on a Pulse Width Modulation (PWM) technique. To control the switching frequency ripple, a front side filter, which can be L, LC, or LCL type, is required. The LCL filter, shown in Fig. 5, is a common option as it can remove high frequency current harmonics.

C. SPECIAL TECHNOLOGIES

Some other AC-DC topologies are shown in Fig. 6. A common single-phase system is based on a diode rectifier combined with a boost converter called single-phase with Power Factor Correction (PFC) as shown in Fig. 6. (a). Its main advantage is the improved line current quality and power factor due to the active circuit in the DC link system. A similar concept has been used in a three-phase diode or controlled rectifier and the topology is called Electronic Inductor [34] as shown in Fig. 6. (b). Its main advantage is the ability to control the DC link current and voltage under different load profiles. The Vienna rectifier shown in Fig. 6. (c) is unidirectional

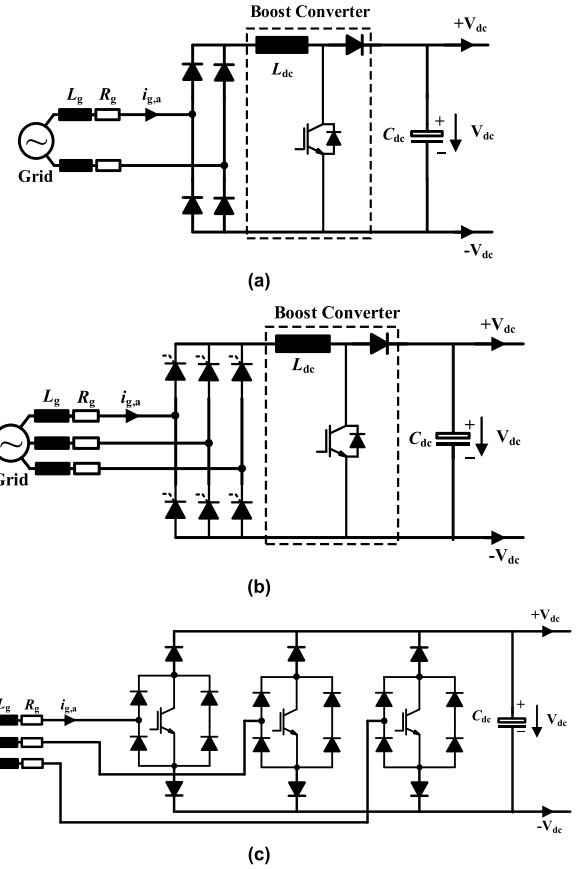


FIGURE 6. AC-DC topologies: (a) single-phase PFC, (b) three-phase EI, and (c) three-phase Vienna rectifier.

with an almost sinusoidal line current. Compared to AFE, less switches are used, meaning lower cost and higher reliability.

IV. ENERGY EFFICIENCY

Improving energy efficiency in the mining industry at both system and equipment levels leads to higher profitability and revenues and a cleaner environment. Authors in [29], [35]–[38] have proposed a hybrid converter system to improve the energy efficiency of high-power mobile mining equipment like shovels and AC draglines. The idea is to store the regenerated power of the equipment in ultra-capacitor banks using a DC-DC converter; this power can then be used for sharing the peak load demand. To improve energy efficiency in mobile mining trucks, the regenerative power can be fed back to the grid using AFE rectifiers and trolley systems [39], [40]. MATLAB simulation and field results demonstrate cost savings, increased production and speed, reduced fleet size, and less emission of greenhouse gases when the trucks operated using these trolley systems. Authors in [20] have demonstrated the relationship between voltage level and energy efficiency of the power system at the terminal of a shovel in a surface mining industry as shown in Fig. 7. It is evident from the graph that addressing the

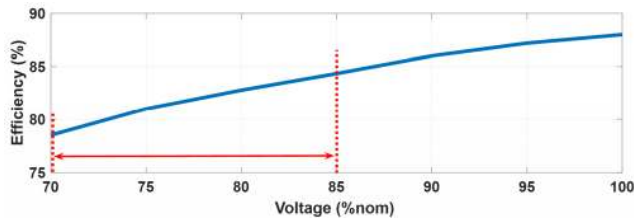


FIGURE 7. Energy efficiency vs voltage regulation at shovel terminals [20].

voltage regulation issue can improve the energy efficiency at the shovel terminals.

Authors in [32] have analyzed the possibility of using an ASD for 6000 hp exhaust dryer fan in a Canadian mining industry with high energy efficiency and economic benefits. Authors in [24]–[28] have also discussed the application of ASDs to improve energy efficiency for ventilation, refrigeration, and cooling systems in different mining industries. Harmonics in a power system are a source of energy wastage leading to inefficiency. Improvement methods in the harmonic filter designs for higher efficiency have been presented in [31], [41]–[44].

Diesel driven trucks are widely used in the mining industry for the transportation of extracted material to dump site, stockpiles, or mineral processing plant. Recent technological advancements related to electric vehicles indicate that electric trucks (eTrucks) in the mining industry will ultimately replace the conventional diesel-driven trucks. With the launch of Tesla Semi eTruck in October 2017, the first eTruck has already entered the market [45]. The latest research reveals that the share of eTruck market could increase to 15% by 2030 due to economic benefits, electrification readiness, and stricter environmental regulations. A comparison between energy consumption of battery eTrucks and buses with conventional diesel-driven ones, performed by California Air Resources Board (CARB), shows that their energy efficiency could be up to six times higher especially in low-speed operations [46]. This outcome is particularly important for mining industries, where the trucks operate at low-speeds with frequent stops for loading and unloading of material. However, authors in [47] have discussed that the commercial use of heavy-duty eTrucks is still not possible due to limited technologies and infrastructure for their recharging along with payload mass and volume constraints. Nonetheless, their widespread commercialization is expected after 2025 due to the great potential of ongoing research and projects in the field of heavy-duty eTrucks.

During recent years, a number of mining industries in Australia, USA, Canada, South Africa, Chile and some other countries have adopted renewable energy solutions to fulfill their energy requirements [9]. Authors in [10] have discussed the possibility of using renewable energy at both system and equipment levels for an open-cut mine. A DC distribution system has been proposed as an alternative to conventional AC distribution systems. Improved stability, higher

efficiency, better power quality, improved voltage regulation, longer trailing cables extending the reach of mobile mining equipment, and higher power delivery at long distances have been mentioned as the advantages of DC distribution systems. They also requiring a smaller number of equipment. One such typical microgrid arrangement for a dragline is shown in Fig. 8.

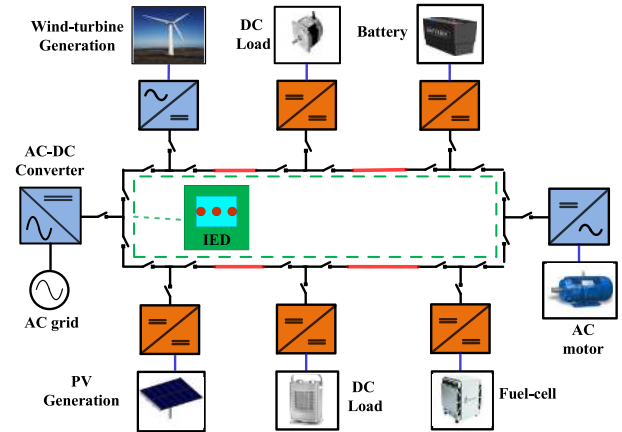


FIGURE 8. A ring-type DC microgrid topology [48].

V. POWER QUALITY ISSUES IN THE MINING INDUSTRY

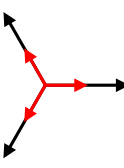
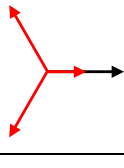
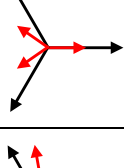
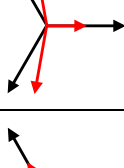
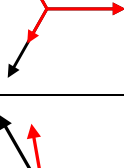
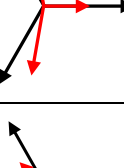
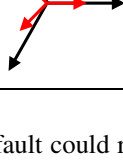
Various power quality problems in electrical distribution system have been reported in [49], [50]. Among them, voltage sag is a common disturbance in industrial distribution network confirmed with recent power quality recorded data. Authors in [51] have discussed the economic impacts of power quality issues on consumers. For that purpose, flicker, voltage unbalance, harmonics, and sags have been analyzed with respect to their economic impacts. Production losses due to interruptions, reinstatement of process parameters, damaged electrical equipment, energy inefficiency, and lower staff productivity are some of the major consequences of these power quality problems. The impact of sags and harmonics are widespread and economically more significant as compared to other power quality issues. A large scale power quality monitoring project known as Power Quality Compliance Audit (PQCA), which has been in progress in Australia since 2002, has been introduced in [52]. The project relies on the data provided by 12 Australian Distribution Network Service Providers (DNSPs) to monitor and report power quality parameters at the utility, network, and site levels. One of the main contributions of this project is the assistance in the development of the Australian standard for voltage levels AS. 61000.3.100 [53]. In the coming sections, some of the major power quality issues faced by the mining industry along with different techniques to mitigate them are discussed.

A. UNDERVOLTAGE/SAGS

The main reason of voltage sag is an increase in load current, which may extend over one to a few hundred cycles [54]. This

short-term increase of load current could be due to start-up of high power motors, transformer inrush current, short-circuit, or fast reclosing of circuit breakers [55]. Many voltage sag incidents occur due to short-circuit events in distribution networks. Possible short-circuit events in a distribution network include three-phase, single-phase-to-ground, phase-to-phase, and two-phase-to-ground faults, discussed as follows [56]. A classification of sag types is summarized in Table 1 and Table 2 summarizes the effect of transformer type on sag characteristic.

TABLE 1. Classification and characteristics of balanced voltage sag types [56].

Type	Voltage vector diagram	Phase voltages (pu)
A		$V_a = V_f$ $V_b = -\frac{1}{2}V_f - j\frac{\sqrt{3}}{2}V_f$ $V_c = -\frac{1}{2}V_f + j\frac{\sqrt{3}}{2}V_f$
B		$V_a = V_f$ $V_b = -\frac{1}{2} - j\frac{\sqrt{3}}{2}$ $V_c = -\frac{1}{2} + j\frac{\sqrt{3}}{2}$
C		$V_a = V_f$ $V_b = -\frac{1}{2} - j\frac{\sqrt{3}}{2}V_f$ $V_c = -\frac{1}{2} + j\frac{\sqrt{3}}{2}V_f$
D		$V_a = V_f$ $V_b = -\frac{1}{2}V_f - j\frac{\sqrt{3}}{2}$ $V_c = -\frac{1}{2}V_f + j\frac{\sqrt{3}}{2}$
E		$V_a = 1$ $V_b = -\frac{1}{2}V_f - j\frac{\sqrt{3}}{2}V_f$ $V_c = -\frac{1}{2}V_f + j\frac{\sqrt{3}}{2}V_f$
F		$V_a = V_f$ $V_b = -\frac{1}{2}V_f - j\frac{\sqrt{3}}{3} - j\frac{\sqrt{3}}{6}V_f$ $V_c = -\frac{1}{2}V_f + j\frac{\sqrt{3}}{3} + j\frac{\sqrt{3}}{6}V_f$
G		$V_a = \frac{2}{3} + \frac{V_f}{3}$ $V_b = -\frac{1}{3} - \frac{1}{6}V_f - j\frac{\sqrt{3}}{2}V_f$ $V_c = -\frac{1}{3} - \frac{1}{6}V_f + j\frac{\sqrt{3}}{2}V_f$

Three-phase fault could result in voltage drop in all three phases by the same amount called balanced or type-A sag.

TABLE 2. Transformation of Voltage Sag through Low Voltage Distribution Transformer [56].

Transformer connections	Sag type on primary side						
	A	B	C	D	E	F	G
YNyn	A	B	C	D	E	F	G
Yy, Dd, Dz	A	D	C	D	G	F	G
Yd, Dy, Yz	A	C	D	C	F	G	F

Single-phase-to-ground is the most common fault in distribution network and could result in voltage amplitude drop in the faulty phase only, called type-B sag. Phase-phase fault is another common fault in distribution network causing change in voltage amplitude and phase angle as the voltage vectors of affected phases move towards each other. This change in voltage is normally represented as type-C sag as shown in Table 1. Type-B sag on primary side of Yd (or Dy, Yz) distribution transformer also leads to type-C sag on secondary side as shown in Table 2. Similarly, type C sag after a Yd (or Dy, Yz) distribution transformer leads to type-D sag, where affected phasor moves outward as shown in Table 2. Finally, two-phase-to-ground fault causes only drop in voltage amplitudes of affected phases commonly represented as Type-E sag as shown in Table 1. Like other unbalanced sags (types B, C and D), the characteristic of Type-E sag changes on the secondary side of distribution transformer resulting in type-F and type-G sags.

Different types of voltage sag can be classified in two categories of balanced (type-A) and unbalanced (types-B, C, D, E, F and G). In both categories, the voltage magnitude remains constant during sag with a rectangular shape. However, in some industrial applications, where a large motor is used, the voltage during sag can have a non-rectangular shape [57]–[59].

Authors in [20] have evaluated power quality and energy efficiency of a practical open pit mine distribution system. Comparison between different topologies of the shovels working at the mine site shows that the DC shovel is the most sensitive to sags and swells, whereas AFE AC drive is the least sensitive. In case of unbalanced sag, the voltage amplitude and phase angle of one or two phases change with respect to the other phase(s) depending on fault type, resulting in three-phase voltage unbalance at the Point of Common Coupling (PCC). Apart from this reason, there are several other reasons for voltage unbalance such as unequal distribution of single-phase load on three-phase power system, asymmetrical transformer winding impedances, and connection of unbalanced and overload equipment to power system [60].

Authors in [61] have discussed the impacts of voltage sags on shovels and drillers in typical open-pit mining industries. The root causes of these conditions have been mentioned as long cables and poor design and selection of transformer and cable ratings. As drillers do not use drives, high starting currents can also contribute towards high voltage drops. Field measurements from different mine sites have indicated severe transient and steady state voltage drops. It has been proposed

to design the transformer and cables by considering voltage drops during maximum power operation and to connect a series active power filter at the secondary of step-down transformers for voltage drop compensation. In [62], voltage sag has been mentioned as a major problem in mining industries particularly due to long power cables supplying power to the mining equipment. A distributed synchronous compensator model with either a PI or a hysteresis controller has been proposed and simulated in MATLAB for a power system of underground mines in India. The simulation results show that both controllers can regulate the voltage and effectively reduce the total harmonic distortion of the system current. The hysteresis controller, however, depicts better results compared to the PI controller.

B. OVERVOLTAGE/SWELLS

In [63] authors have discussed that switching overvoltage incidents in mining industry can cause insulation degradation. To analyze these overvoltage incidents, a simulation model for the vacuum circuit breakers has shown that the transient switching overvoltage can be six times higher than the nominal voltage. To alleviate this problem, controlled switching and surge arresters can be used. The impact of long trailing cables and short circuit capacity on the stability of voltage, particularly in the mining industry has been discussed in [30]. In one instance, auxiliary power supplies of Electric Hydraulic Mining Shovel (EHMS) have been damaged due to overvoltage at the secondary of the auxiliary transformer. The case analysis has shown that a main cause of overvoltage is the parallel resonance between the inductance of the substation transformer and the capacitance of long trailing cables due to switching of AFE rectifiers used in Electric Rope Shovels (ERS). Authors have also identified the need to update the IEEE-519 [64] standard to incorporate resonance related guidelines.

Authors in [23] have analyzed a new method for power transfer to motors using ASDs, particularly in the mining industry. PWM allows to control the motor speed but it has numerous disadvantages like transient overvoltage conditions and high-frequency ground currents, which can damage the cable, motor insulation, and bearings. Hence, utilization of a DC cable from the rectifier to the inverter installed near the motor terminals has been proposed. The results have demonstrated that this technique of power transfer is more economical compared to the traditional method of transferring AC power. It can also eliminate abovementioned problems caused by PWM. However, installing the inverter near motor terminals exposes it to different environmental factors like humidity, high temperature, and higher vibrations, causing its premature failure.

C. HARMONICS

Harmonics lead to degradation of motor insulation and energy wastage in a mine electrical system. In [31], authors have designed a passive harmonic filters for mining applications. Current subharmonics and interharmonics generated by min-

ing cycloconverters need to be attenuated by filtering. High pass and C-type filters could be a good choice due to their lower inrush currents and high attenuation factors at high frequencies. C-type filters need to be tuned for low-frequency harmonics due to lower losses, whereas high pass filters should be used for high-frequency harmonics. Two C-type and six high-pass passive filters have been designed for a grinding mill power plant using three 12-pulse cycloconverters. Simulation results have verified the effectiveness of these filters to minimize the total current harmonic distortion values. Similarly, authors in [65] have discussed that interharmonics generated by cycloconverters can cause overvoltage conditions due to resonances and damage the mining electrical equipment. IEEE-519 [64] defines the limits for odd and even harmonics but not for interharmonics, whereas, IEC-61000-2-4 [66] sets the voltage harmonic limits for industrial plants with voltage levels up to 35 kV and just provides guidelines for treating interharmonics. IEC-61000-3-6 [67] is referred for voltage levels above 35 kV. Consequently, defining some limits for interharmonics is necessary. A summary of different methods for harmonic suppression presented by the authors is shown in Table 3.

TABLE 3. Comparison between harmonic suppression techniques.

Technique	Methodology	Advantages	Disadvantages
Harmonic Cancellation	Input harmonics cancellation by phase shifting the output	Inexpensive Effective Reduced THD	Possibility of large voltage harmonics due to resonance from long cable capacitance
Filters	First- or higher-order filters provide an alternative path to the harmonics	Reduced THD Variety of options and techniques are available	Fundamental losses Voltage drops Higher capital cost
Active Filtering	Generation of anti-harmonics for cancellation of harmonics	Reduced THD	Most expensive Early stages of development

Authors in [65] have demonstrated the application of harmonic cancellation and different types of filters for harmonic reduction in a 75 MVA mining power system with a cycloconverter constituting 30% of the total load. PFC capacitors have been installed at the mine. If a neighboring industry also installs PFC capacitors, it can create a series resonance circuit, which can lead to higher THD_i and capacitor bank failure. Authors in [42] have proposed a True Unit Power Factor (TUPF) AFE rectifier for regenerative multi-motor conveyor drive systems. The existing AFE regenerative rectifier uses three-level space vector modulation; however, it is inefficient due to high power losses in the damper resistors. Moreover, it uses a bulky LCL filter, which can cause resonance problems. Alternatively, the proposed rectifier uses Selective Harmonic Elimination Pulsed Width

Modulation (SHEPWM) with only a line reactor, which can efficiently reduce the input current harmonics up to 50th order. The simulation results confirm improved power quality at the grid side, higher efficiency, and excellent dynamic capability. Similarly, a modified version of a SHEPWM technique for low power, high switching frequency 2-level converters has been proposed in [41] and further been implemented in high-power low switching frequency 3-level converters. In [43], a SHEPWM technique along with an LCL filter has been presented to address the power quality issues for three-level AFE Medium Voltage Drives (MVDs) used in mining industry. The harmonic analysis has shown that the low switching frequency technique in SHEPWM has a better harmonic profile compared to Phase Disposition PWM and can reduce switching loss and improve efficiency. A prototype has also been developed and tested, further justifying the proposed design as per IEEE 519-1992 standard [68].

Authors in [69] have proposed a passive harmonic filter for Indirect Field Oriented Control (IFOC) of medium voltage induction motor three-level drives. The goal of this study was to introduce a harmonic filter without affecting the control system. An LC filter and a controller have been designed and the results were analyzed in Simulink with and without the filter at rated and slow speeds. At both low and rated speeds, the filter introduces torque fluctuations, which can be compensated by adjusting the proportional gain of the current controller. On the other hand, THD values of current and voltage are reduced at the machine terminals. In [70], authors have recommended an alternate five-level NPC type G converter for high-power applications in mining industries. Type G converter requires fewer devices compared with the conventional five-level NPC converters. A Phase Disposition Pulse Width Modulation (PD-PWM) technique has been proposed so the PWM harmonics appear in the form of sidebands at double of the switching frequency and its multiples making it easier to mitigate harmonics. Simulation results show lower THDv and THDi for this converter compared to a three-level NPC converter. Moreover, the type G five-level converter can use low-frequency modulation techniques to improve converter efficiency. Authors have proposed a design and control method of a DC-DC converter employing a passive LCL filter for high-power low-loss applications in mining in [44]. The design approach focuses on high efficiency, high voltage step ratio, lower fault currents, stability, economic aspects, zero reactive power, active power balance, and limiting the voltage across the capacitor in the LCL filter. In the implemented design, the higher step voltage ratio is achieved in the post resonant case. A prototype has also been built and tested by introducing a DC fault to verify the design basis and the robustness of the converter.

Voltage distortion in MV network is introduced by switched mode power supplies used in various loads connected to the LV network [71]. The most dominant voltage harmonics in high- and medium-voltage networks is the 5th harmonic. Although single-phase load generates significant 3rd harmonic, it is barely present in high and medium voltage

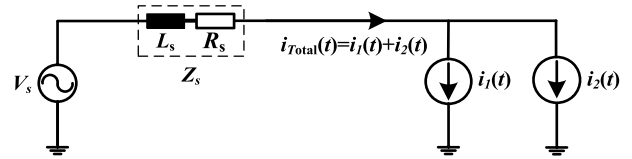


FIGURE 9. A simple model of two current harmonic sources.

networks due to the use of delta-wye transformers in most of low voltage distribution networks. In mining industry, existence of a large number of power converters generate high current harmonics. When combined with grid impedance, they result in voltage distortion at the PCC, which can be seen by other neighbouring converters connected at the same PCC. The diode rectifiers are normally robust against background distortion unless a resonance occurs on any characteristic harmonic of diode rectifier. However, it is important to note that the total current at the PCC is the vector summation of currents generated by different power converters. This fact can be understood by following equations from [72], where two power converters are connected to a sinusoidal voltage source (V_s) with a system impedance (Z_s) as shown in Fig. 9. The n^{th} current harmonics of the two power converters are defined as $i_1(t)$ and $i_2(t)$.

$$i_1(t) = I_1 \sin(\omega_n t + \vartheta_1) \quad (1)$$

$$i_2(t) = I_2 \sin(\omega_n t + \vartheta_2) \quad (2)$$

$$\begin{aligned} i_{tot}(t) &= i_1(t) + i_2(t) \rightarrow I_{tot} \\ &= \sqrt{I_1^2 + I_2^2 + 2I_1I_2 \cos(\vartheta_1 - \vartheta_2)} \end{aligned} \quad (3)$$

where $\omega_n = 2\pi nf$, and ϑ is the phase angle of harmonics. When the grid is not as an ideal source – with low order voltage harmonics below 2 kHz – the grid connected diode rectifiers are not affected significantly. On the other hand, it may even help to reduce the harmonic distortion by harmonic cancellation. Therefore, it is important to consider this idea during harmonic filter selection at PCC.

D. INTERHARMONICS

One of the most complicated subjects recently highlighted in the area of power quality is interharmonics. Interharmonics are spectral components of the voltages and currents that are not multiple integers of the grid main frequency [73]. ASDs [74]–[76], arcing loads [73], [77], [78], static converters [79], and ripple controls [79], [80] are considered the main sources of interharmonics distortions in the grid. Although interharmonics amplitudes are generally lower than integer harmonics, their frequency behavior is much more complex and more difficult to be accurately characterized. Interharmonics could escalate the problems that are already existing due to harmonics and could also result in other problems like light flicker [81], sideband torques on the motor/generator shaft [82], interference with protection signals [83], and dormant resonance excitations [84]. Consequently, interharmonic issue has attracted more attentions recently, and more strict demands have been placed on Power

Electronics products companies to further reduce their interharmonic pollution levels. A major source of interharmonics in the power system is double-stage ASD. In the following subsections, the interharmonics source, identification, and mitigation in ASDs will be elaborated more in detail.

1) INTERHARMONIC SOURCES

Fig. 10 shows the circuit diagram of a double-stage ASD, where the front-end diode rectifier is connected to the rear-end inverter through a DC-link filter, and it feeds the motor at the required power and frequency levels.

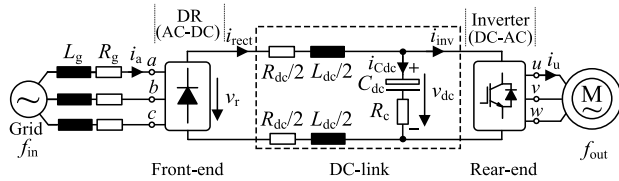


FIGURE 10. Equivalent circuit of an adjustable-speed drive connected to an Induction Motor (IM).

In normal operation of the ASD, its output frequency varies in a wide range. Consequently, the inverter output pulsating voltage is composed of harmonics, which their frequencies depend on the load fundamental frequency f_{out} and the switching frequency f_c . Voltage harmonics (including the fundamental frequency) across the motor load create current harmonics, and accordingly, the harmonical power will be transferred from the inverter output to the DC link. The inverter side current of DC-link (i_{inv}) oscillations will then be affected by the DC-link low-pass filtering function before leaking into the grid [76]. Finally, the rectifier side current of DC-link (i_{rect}) oscillations will then be modulated by the rectifier function and will be injected to the grid. Since the motor frequency f_{out} is usually different from the supply frequency f_{in} , the interactions between the grid harmonics and the oscillations coming from the motor side will give rise to the input current interharmonic distortions. The same scenario may also occur when the input side harmonics are transferred to the inverter side, which can generate interharmonics on the motor side. Prediction of the main interharmonic frequencies may prevent undesirable interference with control and protection signals. Hence, some research works have analyzed the ASDs input current interharmonics frequencies [75], [85].

Notably, in addition to the interharmonic distortions caused by the rectifier and inverter switching operations during normal operating condition, there may be other sources of the interharmonics in ASDs such as the load torque disturbance, the motor shaft eccentricity, and the load current unbalance. From this perspective, variety and complexity of the interharmonics origins have made them one of the most challenging subjects in ASDs.

2) INTERHARMONICS IDENTIFICATION

Interharmonics detection and identification usually suffer from the spectral leakage phenomenon and the picket

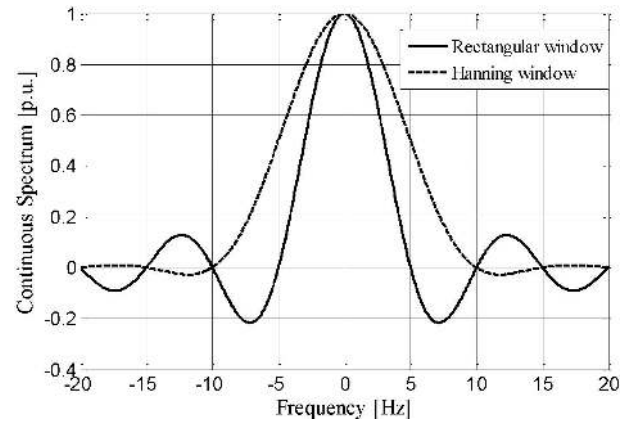


FIGURE 11. Continuous spectrum of Rectangular window (RW) and Hanning window (HW).

fence effect. Therefore, accuracy of the interharmonics analysis highly depends on the precision of the detection approach. The spectral leakage problem may happen if the harmonic components of the signal are not well synchronized with the fundamental frequency. Moreover, adopting a non-suitable windowing period for Discrete Fourier Transform (DFT), where the repetition of the interharmonic components are incomplete, will give rise to the picket fence effect and inaccurate assessment of interharmonics [73], [85]. It is worth noting that the severity of the spectral leakage effects highly depends on the spectral characteristic of the adopted window. Hence, several windowing techniques with quickly decaying side lobes such as Hanning, Hamming and Blackman can be utilized to reduce the leakage effects. Fig. 11 illustrates the spectral characteristics of the Rectangular Window (RW) and Hanning Window (HW). As it can be observed, the HW benefits from better side-lobe behavior compared to RW and it weights suitably the signals, leading to much lower leakage problem.

Harmonics and interharmonics measurement methods and the corresponding results interpretation are recommended in IEC standard 61000-4-7 [86]. It utilizes DFT, which is performed over a rectangular time window of ten cycles for 50 Hz systems, or twelve cycles for 60 Hz systems, corresponding to a time window width of 200 ms. According to the recommendation, a sufficiently high sampling frequency shall also be chosen to allow for analysis of harmonics and interharmonics up to 9 kHz. In this respect, Interharmonic Subgroup (ISG) of amplitude $C_{n+0.5-200-ms}^2$ is defined as given in (4).

$$C_{n+0.5-200-ms}^2 = \sum_{k=2}^8 C_{10n+k}^2 \quad (4)$$

where C_i denotes the rms value of the DFT output as shown in Fig. 12.

Notably, employing the DFT-based identification does not preclude applying other interharmonics estimation approaches such as the parametric and recursive methods [87]. The Prony-based technique and the Estimation

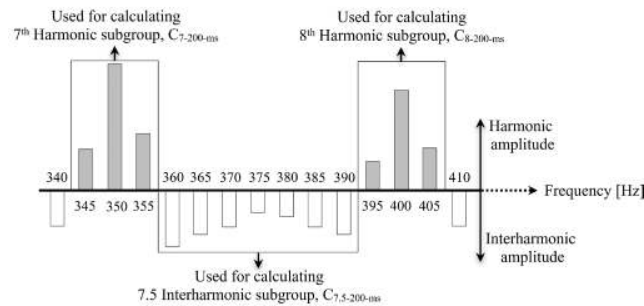


FIGURE 12. Harmonics and interharmonics grouping based on IEC 61000-4-7 [86].

of Signal Parameters via Rotational Invariance Techniques (ESPRIT) are within the most common parametric methods [88], [89]. The estimation precision by employing these approaches strictly depends on the estimation order and the noise interference level. Moreover, the computation burden may increase when higher frequency resolution is required. The recursive method may be generally considered as the parametric method, where there is more knowledge about the given signal. Adopting an appropriate model may have significant effects on the signal parameters estimation in this technique [90], [91].

3) INTERHARMONICS MITIGATION

Interharmonics distortions can highly deteriorate the grid power quality; consequently, the grid operators are passing strict interharmonics rules on the Power Electronic device manufacturers. Accordingly, more attention is given to the interharmonics reduction in double-stage ASD applications [92]. Employing a DC-link active filter has been proposed in several investigations, where the interharmonics generated by the inverter operation and motor are compensated at the DC-link stage [93], [94]. However, the extra costs and the requirement to precise detection of the related harmonics in the DC-link are challenges. In [95], a control approach has been employed in a back-to-back variable drive, where the front-end active rectifier blocks the interharmonic sources in the DC-link. The investigation performed in [96] demonstrates high performance of the Electronic Inductor (EI) based front-end rectifiers in reducing the ASD input current interharmonic components. In this drive, the EI makes the DC-link acting as a high impedance buffer against the oscillations coming from the inverter side.

Although many investigations have been devoted to mitigating the interharmonics after creation, the detection of the interharmonics source and adopting a suitable strategy can reduce interharmonics generation. In this regard, a comprehensive investigation has been conducted in [97], where influence of the most commonly used modulation techniques was highlighted. According to this study, Discontinuous Pulse Width Modulation technique could create higher input current interharmonics compared to the Space Vector Modulation.

E. SUPRAHARMONICS

Authors in [98] have discussed that grid integration of solar and wind powers results in higher harmonics. Low-frequency resonances and reduction in efficiency are some related challenges. So, active, passive, and hybrid type filters are important for the harmonic mitigation and can be installed at on- and off-shore locations. Passive filters, however, can only limit a few harmonics and due to some uncertainties related to models and lack of data, they might be over-sized. On the other hand, active filters can be tuned to control THD and power factor and reduce the uncertainties risk. However, they have the drawback of introducing high-frequency distortions, which can introduce unwanted resonance conditions in case of PV inverters.

In [99] authors have emphasized the importance of studying supraharmonics, primary and secondary emissions, and the need to improve the existing standards and harmonic assessment techniques. Different standards and their limitations have been discussed. IEC 61000-3-2 underlines testing the equipment under sinusoidal conditions but the harmonic emission increases considerably when the voltage is distorted and grid impedance is present. For example, IEC-61400-21 considers the wind turbines as ideal current sources, which do not include the impact of internal and grid impedances. Consequently, the future revision of that standard needs to reflect this impact and specify methods for voltage and phase angle measurements. Authors have studied the phenomena of primary and secondary emissions for the case of supraharmonics in [100]. Harmonic currents of an electric vehicle (EV) connected with a TV, LED, and microwave have been analyzed during EV charging. The study shows that the emissions at the Point of Connection (PoC) can be different from the individual emissions and, hence, the source of emissions cannot be determined without a detailed analysis. As a result, a full-scale model of a home was developed in a lab and primary and secondary emissions due to these devices with and without the presence of EV were measured to prove the existence of secondary emission. It is also possible that some emissions might not travel to other equipment.

Authors in [101] have reviewed different methods of supraharmonics measurement and devised a new high-pass filter design to improve the accuracy, reliability, and signal-to-noise ratio (SNR) above 2 kHz. A transfer function of a filter from the elliptic family has been developed and implemented by producing a prototype analog filter design consisting of passive elements and a digital filter with DSP. The prototype analog filter improves the SNR both in a laboratory and a public LV grid. The laboratory and public LV grid results of the analog and digital filters are consistent.

In [33], authors have proposed to use a Random Pulse Position Modulation (RPPM) technique to reduce supraharmonics emissions in two- and multi-level converters. Measurement, standardization, and analysis of supraharmonic emissions is an area of interest due to the application of 2 to 150 kHz frequency range in Power Line Communication (PLC) and different power electronic devices. Simulation

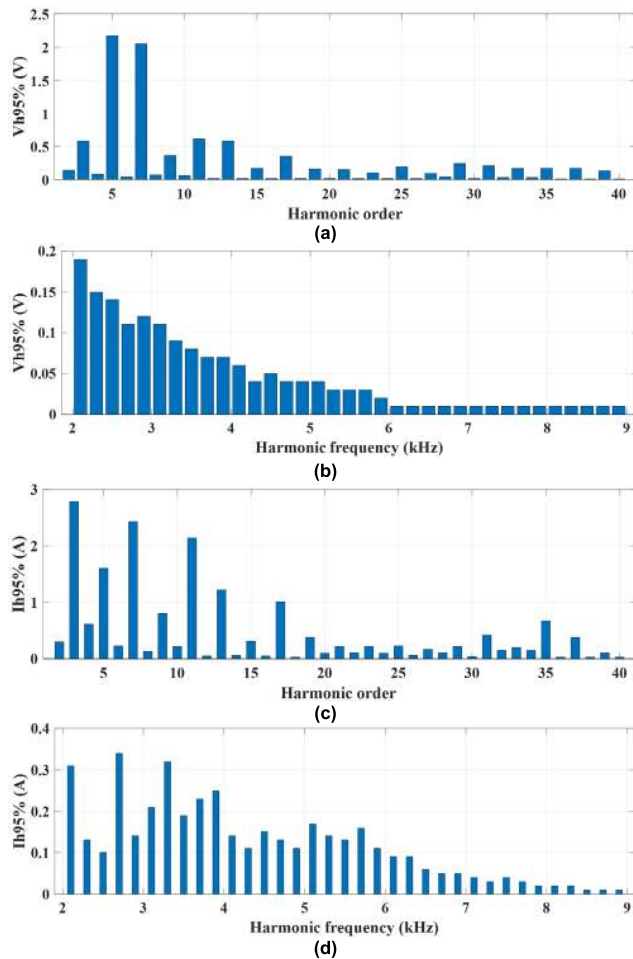


FIGURE 13. 95 percentile values of voltage harmonics over May 2018, for (a) 50-2500 Hz, and (b) 2-9 kHz, and current harmonics for (c) 50-2500 Hz, and (d) 2-9 kHz.

results show that the use of multi-level inverters reduces the supraharmonics emissions compared to two-level inverters. In RPPM, the delay time of the on-pulse from the beginning of the switching period is randomly varied. Simulation results of two- and three-level NPC inverters using this technique show lower voltage and current harmonics at the multiples of switching frequency.

Measurement and analysis of the power quality and supraharmonics of PV inverters have been done using PQ analysers and MATLAB [102], [103]. The devices measure voltage and current harmonic data for 50-2500 Hz and 2-9 kHz ranges, and voltage harmonics 10-150 kHz. Two meters were installed at the outputs of grid-connected PV inverters. Voltage and current harmonics data for a month from both meters have been plotted and reported. The current and voltage harmonics (95 percentile values) for May 2018 for one of the meters are shown in Fig. 13 as an example. Data analysis shows that the voltage harmonics are more significant during day compared to night. That is, higher usage of non-linear loads during day increases harmonics emissions. These results also depict the existence of high voltage harmonic

distortions (up to 13V at 2 kHz) due to resonances particularly in the frequency range up to 9 kHz. The root cause of these resonances might be the excitation of cables capacitance by the harmonics generated by non-linear power electronic loads.

VI. RELIABILITY AND ROBUSTNESS

In the mining industry, the reliability of the electrical power system is important as even a short interruption in power supply can lead to huge production loss, especially when the mining materials are precious like gold and platinum. In [104], it has been proposed to use an advanced fault-tolerant current control of five-phase Permanent Magnet Synchronous Motor (PMSM) for mining applications. PMSM can work reliably under fault conditions using Decoupled Motor Model (DPC) and non-linear Sliding Mode Control (SMC) as a prototype shows. The experimental results show the motor has low distortion sinusoidal phase currents. The motor has constant quadrature and direct axis currents, constant EMFs, ripple-free torque and smooth speed profile during the phase loss.

Authors in [11] have discussed that voltage and frequency variations could lead to commutation failure of cycloconverters used in the mining industry. Consequently, the maximum bearable voltage drop at the converter input terminals needs to be identified. Then, a case-study in a 15 MW cycloconverter shows that voltage drops greater than 20% could cause commutation failure. Hence, to improve the system reliability, the maximum voltage drop, and frequency variation need to be considered and suitable under-voltage and under-frequency protection settings must be adjusted.

In [22], authors have discussed different topologies for medium voltage converters and proposed the usage of three-level Fault Tolerant Active Neutral Point Clamped Voltage Source Converter (FT ANPC VSC) to improve the reliability of a mine hoist electrical system. Simulation indicates that the junction temperature in ANPC mode is less than NPC mode, leading to lower thermal stress and longer lifetime. Practical results from a prototype FT-ANPC have confirmed the improved lifetime of these converters. The reconfiguration capability of FT-ANPC along with prognostic methods have been also demonstrated. The grid disturbances can have impacts on ASD in terms of performance and reliability as shown in Fig. 14. In the following sections, major effects of grid disturbances on three-phase ASD with a diode rectifier topology have been analyzed.

A. INPUT VOLTAGE SAG, UNDERVOLTAGE AND UNBALANCE

Voltage sag could cause fluctuation in DC link voltage of ASD. In that case, ASD tries to stabilize the load power by adjusting the modulation index. Thus, line and DC link currents could be affected and operate outside their safety zones. The higher current magnitude could saturate inductors, resulting in higher ripples in the line current, which has a negative impact on the capacitor lifetime and protection of the

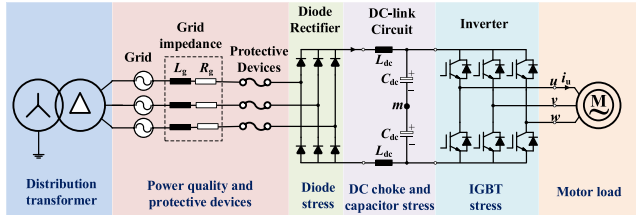


FIGURE 14. Negative impacts of grid disturbances on ASD operation.

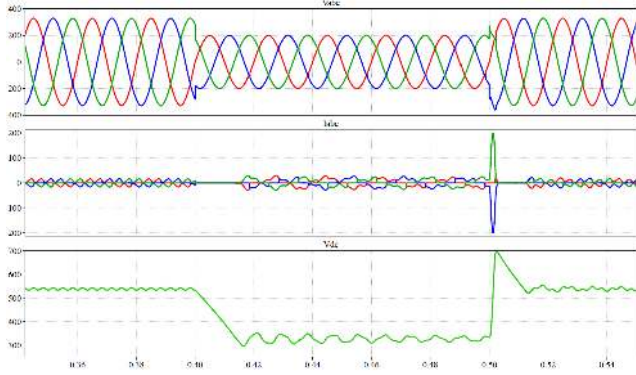


FIGURE 15. Operation of ASD with 30% voltage sag (Type-A): three-phase line voltage and current, and DC-link voltage waveforms.

ASD system. Furthermore, the impact of voltage sag on ASD operation depends on the sag characteristics. For example, during balanced voltage sag (type-A), the DC-link voltage significantly drops due to the drop in all three-phase line voltages. However, the scenario can be totally different in unbalanced voltage sags due to different phases having different voltage drops. It has been shown in [105] that balanced sag (type-A) is more destructive than other sag types, as the maximum AC voltage no longer exceeds the DC-link voltage as shown in Fig. 15; thus, the DC-link capacitor continues to discharge, which leads to drop in DC-link voltage and increase in the current, which can stress the IGBT module. However, duration of decay in DC-link voltage depends on the magnitude of sag and load connected to the DC bus. The voltage drop in balanced sag can result in a drop in motor terminal voltage causing a drop in torque and, consequently, a reduction in motor speed.

The impact of balanced and unbalanced sags on ASD operations in term of DC-link voltage drop and AC current peaks has been analyzed in [106]. It has been confirmed that balanced sag Type-A has the worst consequence on the DC-link voltage, whereas unbalanced sag Type-B has the least consequence on this parameter. However, estimating the behavior of ASD during unbalanced sag is more complicated due to significant ripples in the DC-link voltage and input line current as shown in Fig. 16.

The voltage unbalance and asymmetrical voltage sag affect the ASD operation in the same way. Most of asymmetrical sags result in changing the voltage amplitude and its phase jump. However, it has been indicated in [107] that jump in

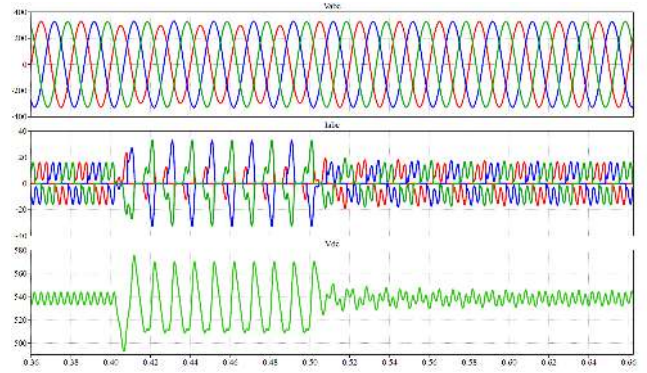


FIGURE 16. Operation of ASD with 30% voltage sag (Type-B): three-phase line voltage and current, and DC-link voltage waveforms.

phase-angle does not have any significant impact on ASD operation. One of the major effects of unbalanced voltage on ASD is that the DC-link capacitor discharges more than a normal amount as the energy is still being fed through the inverter to the motor load. Thus, when the un-sagged (healthy) input voltage phase forward biases the diode rectifier to supply all the energy and recharges the DC-link capacitor, a large amount of current flows in that phase. During unbalanced voltage sag, three-phase diode rectifier is forced to enter in single-phase operation. However, this behavior does not depend on sag level, but on line impedance, DC-link choke and capacitor [54]. The single-phase operation of drive degrades the input power factor and current Crest Factor (CF), and creates significant line current peak; they can stress the diode bridge rectifier and input protective devices such as circuit breakers and fuses [108].

Normally, the rectifier diodes are already operating at their rated current level when the ASD is delivering 50% rated power during single-phase rectifier operation [109]. To estimate the input current unbalance due to voltage unbalance, a relationship has been developed by using analytical approach in [110]. Operation of three-phase diode rectifier under unbalanced condition could result in 6-pulse, 4-pulse, or 2-pulse mode operation, depending on voltage unbalance and drive configuration [110]. The unbalance factor of fundamental current (μ) can be defined as the ratio of negative over positive sequence currents (I_n/I_p), given for 6-, 4-, and 2-pulse operation modes in (5), (6), and (7) respectively [110].

$$\mu = \frac{\sqrt{3}}{2\rho} u \quad (5)$$

$$\mu = \sqrt{c^2 \left(\frac{u}{\rho}\right)^2 + \frac{1}{\sqrt{3}} c \frac{u}{\rho} + \frac{1}{3}} \quad (6)$$

$$\mu = 1 \quad (7)$$

where c is the phase angle of deviated line voltage, $\rho = V_r / \sqrt{2} V_p$ is voltage drop ratio, V_p is the line voltage peak, V_r is peak-to-peak of the rectifier voltage, and $u = V_n/V_p$ is voltage unbalance factor (V_n is the negative sequence

voltage magnitude). High line current harmonic from ASD also deteriorates the performance of the transformer. Transformer K-factor in (8) is used as a measure of additional losses due to harmonics.

$$K = \sum_{h=1}^{h=h_{max}} I_h^2 h^2 \quad (8)$$

where, I_h is the RMS current amplitude of harmonic h . K-factor is a derating factor for a transformer and indicates its suitability to be used with loads with non-sinusoidal currents [108], [111] and is useful for specifying transformers that are connected to nonlinear loads such as ASD system. It has been shown that CF, power factor, and K-factor do not vary much with the amount of voltage sag or unbalance, once the front-end rectifier enters single-phase operation [108]. That operation mode of three-phase front-end rectifier under unbalanced condition generates low-order even harmonic voltages in the DC-link voltage [107]. They can significantly raise the AC-flux densities of the core material of DC-choke compared with normal balanced condition; this will cause additional core losses and can saturate the DC-choke. The effects of low-order harmonics on magnetic flux densities can be understood by following equations [107].

$$B_{dc} = \frac{(3.19)NI_{dc}}{(0.85)l_g} [Tesla] \quad (9)$$

$$B_{ac(h)} = \frac{V_h \times 10^8}{(4.44)f_h A_c N \cdot SF} [Tesla] \quad (10)$$

$$B_{pk} = B_{dc} + B_{h=100Hz} + B_{h=300Hz} [Tesla] \quad (11)$$

where, B_{dc} is DC flux density, $B_{ac(h)}$ is AC flux density due to voltage harmonics, B_{pk} is peak core flux density, l_g is air-gap length, N is the number of winding turns, I_{dc} is DC-link current flowing through choke, V_h is the ac harmonic component in DC-link voltage at f_h frequency, A_c is core cross-sectional area, and SF is the core stacking factor. Equation (11) shows how these harmonics generated due to voltage unbalance can cause a rise in peak operating flux density (B_{pk}) in the core of DC-choke.

The ASD DC-link capacitors are commonly electrolytic. These capacitors have rather high Equivalent Series Resistance (ESR), which is a function of temperature and frequency. A high ripple current under unbalanced conditions can further increase ESR value. Also, it is important to note that the capacitor ESR increases significantly at low frequencies, therefore capacitor losses are extremely high at low frequency components (i.e 100Hz, 200Hz and so on) [112]. The total power loss in the DC-link capacitor can be calculated by using RMS value of the capacitor harmonic current (I_{ch}) as given in (12).

$$P_{loss} = \sum_{h=1}^{h=n} I_{ch}^2 ESR(f_h) \quad (12)$$

The total power loss can then be used to determine the capacitor hot spot temperature (T_h) and then operating lifetime (L_{op})

of DC-link capacitor as follows [113].

$$T_h = T_a + P_{loss} R_{th} [C] \quad (13)$$

$$L = L_o 2^{\frac{T_o - T_h}{p_2}} \left(\frac{V}{V_o} \right)^{-p_1} [Hours] \quad (14)$$

where L_o , V_o , V , R_{th} , T_o and T_h are the rated lifetime, rated voltage, real voltage, capacitor thermal resistance, ambient temperature, and hot-spot temperature respectively. The coefficients p_1 and p_2 for any specific capacitor can be selected from [114]. The harmonics in DC-link voltage due to line asymmetrical voltage sag/unbalance can distort the PWM output voltage of inverter and cause harmonics currents in the motor load. The harmonics in motor currents create ripple in motor torque at the same frequency as seen in DC-link voltage, known as pulsating torque [115]. The motor line-to-midpoint voltage (V_{um}) under balanced condition is as given in (15).

$$V_{um}(\omega_o t) = \frac{1}{2} V_{dc}(t) A_1 \sin(\omega_o t) \quad (15)$$

where, ω_o is the inverter output frequency and A_1 is the Fourier coefficient. The DC-link voltage of ASD under voltage sag and unbalanced condition is as given in (16).

$$V_{dc}(t) = V_{dc} + \sum_{h=2}^n V_{dch} \cos(2\omega_s t + \phi_h) \quad (16)$$

where, V_{dc} is the average value of DC-link voltage, V_{dch} is the amplitude of the voltage harmonic component at harmonic order h , and ω_s is the supply frequency from grid. The motor line-to-midpoint voltage (V_{um}) under sag/unbalanced conditions is as given in (17).

$$V_{um}(\omega_o t) = \frac{1}{2} V_{dc}(t) A_1 \sin(\omega_o t) + \sum_{h=2}^n \left[\frac{1}{4} V_{dch} A_1 (\sin(2\omega_s t + \omega_o t + \phi_h) - \sin(2\omega_s t - \omega_o t + \phi_h)) \right] \quad (17)$$

The ripple in DC-link voltage are dominated by second order harmonic, therefore (17) can be simplified by considering only the second order harmonic as given in (18).

$$V_{um}(t) = \frac{1}{2} V_{dc}(t) A_1 \sin(\omega_o t) + \frac{1}{4} V_{dc2} A_1 [\sin((2\omega_s + \omega_o)t + \phi_2) - \sin((2\omega_s - \omega_o)t + \phi_2)] \quad (18)$$

Under sag/unbalanced conditions, the motor phase current $I_u(t)$ is given in (19) and instantaneous torque T_e is given in (20). Details of derivation of these parameters are provided in [107].

$$I_u(t) = I_{s0} \cos(\omega_o t + \phi_o) + I_{s1} \cos(2\omega_s t + \omega_o t + \phi_1) + I_{s2} \cos(2\omega_s t + \omega_o t + \phi_2) \quad (19)$$

$$T_e = T_{e0} + T_{e2} \cos(2\omega_s t + \phi_2) + T_{e4} \cos(4\omega_s t + \phi_4) \quad (20)$$

Equation (20) includes an average DC term (T_{e0}) contributed by balanced three-phase supply, and pulsating torque components (T_{e2} and T_{e4}) at the same ripple frequency as seen in DC-link voltage (i.e. at 100Hz and 200Hz). A question might be raised that whether ASD configuration with AC choke or DC choke can give any difference in ripple components of DC-link voltage and then pulsating torque. It has been shown in [116] that the placement of inductor on any specified location gives almost identical performance as long as DC choke inductor is twice the value of each AC line inductor. The resulted pulsating torque created due to voltage sag/unbalance can give undesirable effects to motor load in term of vibration and audible noise [116], [117]. However, an advanced motor control algorithm like Rotor-field Oriented (RFO) or Direct-Torque Control (DTC) can be used to mitigate the pulsating torque [117].

B. INPUT VOLTAGE SWELL, OVERVOLTAGE AND TRANSIENT

The main causes of voltage swell, overvoltage, and transient in distribution systems are as follows.

- In case of isolated or high resistance grounding systems used in mining industry, a single line-to-ground fault on the system results in a temporary voltage rise on the healthy phases.
- Voltage swell or overvoltage can also be generated by sudden load variation in the system. The quick disruption of current can generate a large voltage ($V = L di/dt$).
- Switching on a large distribution capacitor bank can also cause a swell, however swell mainly has an oscillatory transient nature.
- Ferroresonance is another reason of voltage swell or transient in the system and mainly occurs due to a special form of series resonance between the magnetizing inductance of transformer and the distribution/system capacitor.

In ASD, the rectifiers are uncontrolled, therefore DC-link voltage follows the changes of the AC line voltage. The DC-link filter tries to perform the same function irrespective of change in the voltage, but the overvoltage results in higher AC ripple at DC bus, which may saturate the DC-link filter inductor and abolish its effects. Although the ASD drives have several protective functions such as overvoltage and overcurrent, sometime the transients result in dangerous rises in voltage level. As this rise can be quicker than protective functions reaction time, it can damage the inverter transistors and the DC-link capacitor. This impact can be understood from (13), where the DC-link capacitor lifetime depends on operated voltage (V_O). Apart from ASD, other connected electronic and sensitive equipment in the installation may be damaged or be prone to malfunction due to overheating caused by overvoltage.

C. INPUT COMMUTATION NOTCHES

In mining industry, a number of silicon-controlled rectifiers (SCRs) or thyristor bridges DC drives are used. Although the gate firing angle of the SCR can be adjusted to control the level of DC link voltage, it generates voltage notches during commutation period [118], [119]. Nowadays, AC drives are replacing DC drives due to their better reliability and efficiency. However, still there are numerous customer sites, where many DC drives are in operation and connected with diode rectifier-based AC drives to the same distribution network. Recently, a number of AC drive trips and components failures have been reported on such customer sites and it has been confirmed that they are due to input voltage notches generated by DC drives [120], [121]. Operation of ASD under commutation notches can result in higher frequency harmonic contents and voltage surges, which can lead to control and instability problems in ASD. These high frequency harmonics generated by commutation notches could be a major concern where multiple drives are connected to the PCC.

VII. POWER QUALITY ANALYSIS OF MINING DISTRIBUTION NETWORK: A CASE STUDY

For this study, a mining distribution system has been considered where Bulk Miner, Auxillary Miner, and Collecting Machine consist of a large number of power converters loads (motor drives) in the form of Pump (P), Wheel (W), and Cutter Head (CH), which are connected via a step down transformer as shown in Fig. 17 (a). In actual mining system, other auxillary loads are also connected to the system, but in this study, the main focus is only power electronic loads. Three-phase diode or SCR rectifiers with either a large electrolytic DC-link capacitor and a DC or an AC choke, or a Small DC-Link Capacitor (SLDC) shown in Fig. 17 (b) are commonly used in mining application.

A mining distribution system with n, m, and k numbers of parallel-connected SLDC, DC choke, and AC choke is modelled as shown in Fig. 18.

In this study, interconnection impedances between the power converters are assumed to be negligible and the distribution transformer (T) is defined as the major inductive impedance (L_g) of the system at the grid side as shown in Fig. 18. The total impedance of the system is calculated based on three paralleled group of power converters topologies in series with the line inductance as given in (21) [122].

$$Z_{in} = j(2\omega L_g) + \left(\frac{1}{j\omega(nC_{small}) + \frac{n}{R_{load}}} \parallel \frac{1 - 2\omega^2 L_{dc} C_{dc} + j\omega \frac{2L_{dc}}{R_{load}}}{j\omega(mC_{dc}) + \frac{m}{R_{load}}} \right) \times \frac{1 - 2\omega^2 L_{ac} C_{dc} + j\omega \frac{2L_{ac}}{R_{load}}}{j\omega(kC_{dc}) + \frac{k}{R_{load}}} \quad (21)$$

To analyze the impact of different combinations of power converter topologies, six different combinations as given in Table 4 have been considered to study the mining

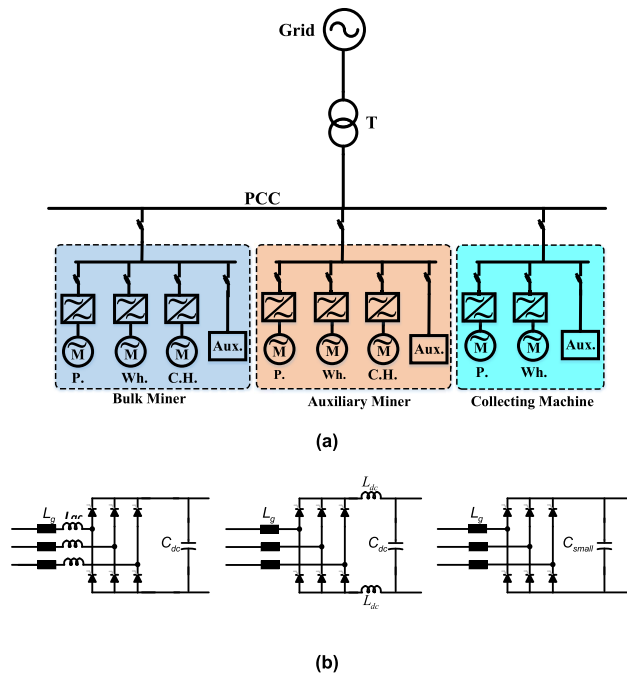


FIGURE 17. (a) Mining distribution network, (b) three-phase power electronic converters with AC choke, DC choke and SLDC rectifier.

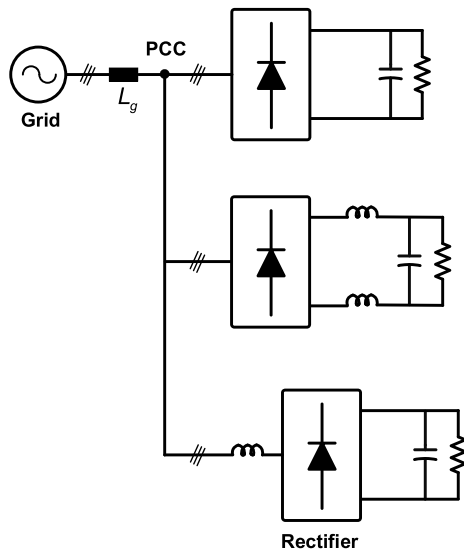


FIGURE 18. Mining distribution system with different groups of power converters topologies connected at the PCC.

distribution system of Fig. 18. Different combinations of power converter topologies will create different resonant frequencies in the distribution system as shown in Fig. 19.

In this analysis, conventional power converters used same size of DC-link capacitor and filter inductor (either on AC or DC side), therefore impedance curve is exactly the same for cases 1 and 2. However, the resonant frequency shifts above 100Hz in case 3, where all 9 converters are SLDC. Another interesting observed fact is that the second resonant frequency varies with change in number of SLDC converters. This is due to the fact that SLDC converters have around one-fifteenth

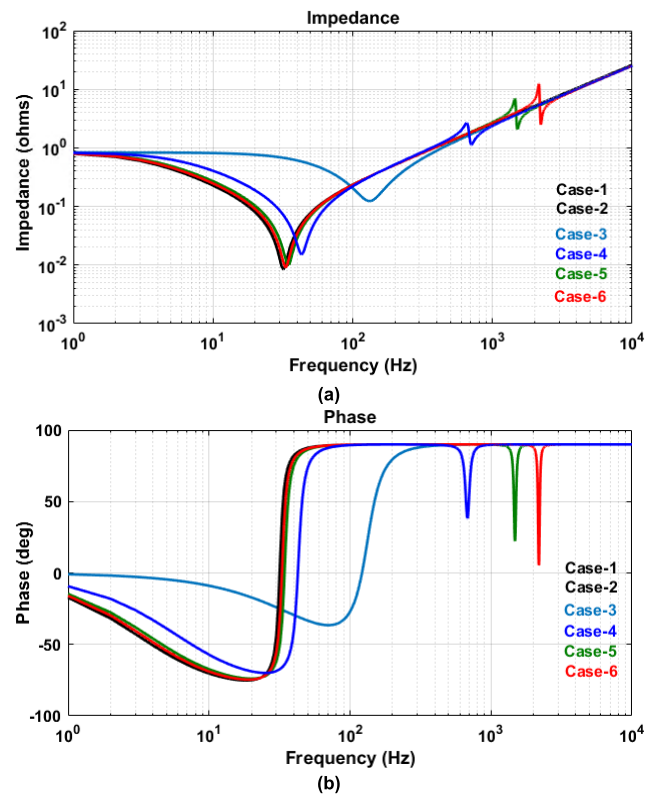


FIGURE 19. Mining distribution network impedance (a) magnitude, (b) phase angle.

TABLE 4. Different combinations of the power converters.

Power Converter Groups			
Case	DC Choke (m)	AC Choke (k)	SLDC (n)
1	9	0	0
2	0	9	0
3	0	0	9
4	3	3	3
5	4	3	2
6	7	1	1

of DC-link capacitance compared to conventional converters (with AC choke or DC choke). Therefore, at the system level, the second resonant frequency occurred in higher frequency area due to combination of SLDC converters as can be seen in cases 4, 5, and 6.

This analysis shows that if a nonlinear load generates higher frequency current harmonics due to system resonance (such as SLDC converters in this study), they may circulate through other loads, and hence affect the voltage quality at the PCC. For example, in cases 4 and 6, second resonant frequencies occurred around 1kHz and 2kHz respectively due to different combination of converter topologies. In both cases, harmonic performance at PCC will be different due to resonance frequency as shown in Fig. 20, where the impact of resonance frequency can be clearly seen at 19th harmonic (950Hz) and 37th harmonic (1850Hz).

Thus, in mining application, where system configuration is very complex, it is important to highlight that:

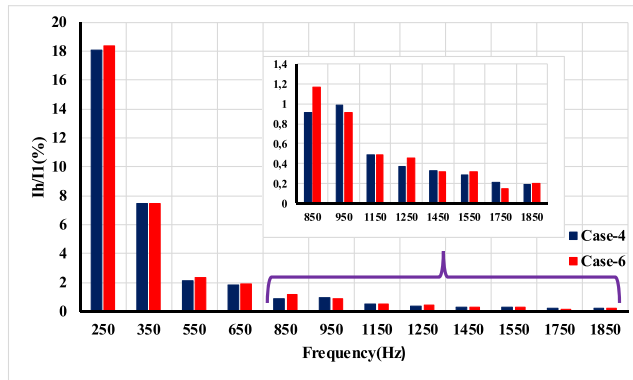


FIGURE 20. Harmonic emission of power converter for case-4 and case-6.

- The harmonic emission and performance of any non-linear load connected to a low distribution network are influenced by grid impedance. If grid impedance has resonant frequencies in higher frequency range the overall quality of the system cannot be estimated based on the harmonic performance at the product/unit level.
- Performance of some converter topologies such as SLDC is highly influenced by grid impedance. The distortion in higher frequency range may be significant, especially in 2kHz onward. Even though, there is no general regulation and compatibility levels for higher frequency harmonics (2kHz onward) at this moment, but different standard organizations have already started working on the definition of compatibility levels for the frequency range of 2-150kHz.
- In order to select harmonic mitigation techniques at PCC, it is important to have detail information about connected loads, their configuration, transformer, and cable size. There is a possibility of multi-resonance phenomenon due to different topologies of power converters.
- Multi-resonance phenomenon not only affect power quality at PCC but also, at the same time, can create severe reliability and life-time issues for the power converters, distribution transformer, and other connected equipment at the PCC.

VIII. CONCLUSION

This work reviews the current state of distribution networks in mining industry with focus on challenges in the areas of system robustness, energy efficiency, and power quality. After describing general characteristics of different types of mining power systems, the most common topologies of power electronics in the industry along with their benefits and limitations are presented. Next, recent efforts to improve the energy efficiency of mining networks have been mentioned. Major challenges in the areas of power quality in the mining industry are undervoltage, overvoltage, harmonics, interharmonics, and recently supraharmatics. Several research and industry cases covering these issues along with proposed solutions are

presented in this paper. Finally, reliability and robustness of mining systems have been explained and evaluated.

ACKNOWLEDGMENT

The authors acknowledge the Australian Research Council, supporting FT150100042, LP170100902, and LP160101675 projects.

REFERENCES

- [1] G. Agricola, *De Re Metallica*. New York, NY, USA: Dover, 1950.
- [2] Australian Science and Technology Heritage Centre. (2000). *A Condensed History of Australian Technological Innovation and Adaptation During the First Two Hundred Years/Compiled by Fellows of the Australian Academy of Technological Sciences and Engineering*. [Online]. Available: <https://nla.gov.au/nla.cat-vn3084879>
- [3] Department of Industry Innovation and Science. (Oct. 24 2017). *Annual Report 2016-2017*. [Online]. Available: <https://industry.gov.au/AboutUs/CorporatePublications/AnnualReports/AnnualReport201617/Annual-Report-2016-17.pdf>
- [4] Department of Industry Innovation and Science. (Mar. 2018). *Industry Insights: Flexibility and Growth 1/2018*. [Online]. Available: <https://industry.gov.au/Office-of-the-Chief-Economist/Publications/IndustryInsights/documents/Industry-Insights-Flexibility-and-growth.pdf>
- [5] T. Novak, J. Sottile, and B. Brusso, "Mine electrical systems, part 1 [history]," *IEEE Ind. Appl. Mag.*, vol. 21, no. 5, pp. 7–13, Sep./Oct. 2015.
- [6] J. Sottile and T. Novak, "Mine electrical systems, part 2-alternating current systems [History]," *IEEE Ind. Appl. Mag.*, vol. 21, no. 6, pp. 8–13, Nov./Dec. 2015.
- [7] *Electrical Equipment for Mines and Quarries AS/NZS Volume 4871.1*, Standards Australia, Sydney, NSW, Australia, 2012.
- [8] P. Darling and M. Society for Mining, and Exploration, *SME Mining Engineering Handbook*, 3rd ed. Englewood, CO, USA: Society for Mining, Metallurgy, and Exploration, 2011.
- [9] *Database: Solar & Wind Systems in the Mining Industry*. Accessed: Sep. 2019. [Online]. Available: <https://www.th-energy.net/english/platform-renewable-energy-and-mining/database-solar-wind-power-plants/>
- [10] M. G. Jahromi, G. Mirzaeva, S. D. Mitchell, and D. Gay, "Powering mobile mining machines: DC versus AC power," *IEEE Ind. Appl. Mag.*, vol. 22, no. 5, pp. 63–72, Sep./Oct. 2016.
- [11] G. F. Silva, T. L. Morán, T. M. Torres, and V. C. Weishaupt, "A method to evaluate cycloconverters commutation robustness under voltage and frequency variations in mining distribution systems," *IEEE Trans. Ind. Appl.*, vol. 54, no. 1, pp. 858–865, Jan./Feb. 2018.
- [12] P. A. Aravena, L. A. Morán, R. Burgos, P. Astudillo, C. Olivares, and D. A. Melo, "High power cycloconverter for mining applications: Practical recommendations for operation, protection and compensation," *IEEE Trans. Ind. Appl.*, vol. 51, no. 1, pp. 82–91, Jan./Feb. 2015.
- [13] P. Stepien and R. Griffiths, "History of earthing and the impact on coal mining," in *Proc. Down Earth Conf. (DTEC)*, Sep. 2016, pp. 1–6.
- [14] *IEEE Recommended Practice for Grounding of Industrial and Commercial Power Systems—Redline*, Standard IEEE 142-2007, 2007, pp. 1–215.
- [15] J. Sottile, T. Novak, and A. K. Tripathi, "Best practices for implementing high-resistance grounding in mine power systems," *IEEE Trans. Ind. Appl.*, vol. 51, no. 6, pp. 5254–5260, Nov./Dec. 2015.
- [16] T. Novak, "The effects of very-high-resistance grounding on the selectivity of ground-fault relaying in high-voltage longwall power systems," *IEEE Trans. Ind. Appl.*, vol. 37, no. 2, pp. 398–406, Mar. 2001.
- [17] T. Novak, "Analysis of very-high-resistance grounding in high-voltage longwall power systems," *IEEE Trans. Ind. Appl.*, vol. 37, no. 1, pp. 104–111, Jan. 2001.
- [18] T. Novak, J. Basar, J. Sottile, and J. L. Kohler, "The effects of cable capacitance on longwall power systems," *IEEE Trans. Ind. Appl.*, vol. 40, no. 5, pp. 1406–1412, Sep. 2004.
- [19] J. Sottile, S. J. Gnappagasam, T. Novak, and J. L. Kohler, "Detrimental effects of capacitance on high-resistance-grounded mine distribution systems," *IEEE Trans. Ind. Appl.*, vol. 42, no. 5, pp. 1333–1339, Sep. 2006.
- [20] P. Aqueveque, E. P. Wiechmann, J. A. Henríquez, and L. G. Muñoz, "Energy quality and efficiency of an open pit mine distribution system: Evaluation and solution," *IEEE Trans. Ind. Appl.*, vol. 52, no. 1, pp. 580–588, Jan./Feb. 2016.

- [21] R. N. Fard and E. Tedeschi, "Investigation of AC and DC power distributions to seafloor mining equipment," in *Proc. OCEANS*, Jun. 2017, pp. 1–7.
- [22] V. N. Ferreira, G. A. Mendonça, A. V. Rocha, R. S. Resende, and B. J. C. Filho, "Medium voltage IGBT-based converters in mine hoist systems," in *Proc. IEEE Ind. Appl. Soc. Annu. Meeting*, Oct. 2016, pp. 1–8.
- [23] V. C. D. Paula and H. D. Paula, "Employing DC transmission in long distance AC motor drives: Analysis of the copper economy and power losses reduction in mining facilities," *IEEE Trans. Ind. Appl.*, vol. 54, no. 1, pp. 841–847, Jan./Feb. 2018.
- [24] P. Maré, C. J. R. Kriel, and J. H. Marais, "Energy efficiency improvements through the integration of underground mine water reticulation and cooling systems," in *Proc. Int. Conf. Ind. Commercial Energy (ICUE)*, Aug. 2016, pp. 112–117.
- [25] A. J. Schutte, M. Kleingeld, and L. Van der Zee, "An integrated energy efficiency strategy for deep mine ventilation and refrigeration," in *Proc. Int. Conf. 11th Ind. Commercial Energy*, Aug. 2014, pp. 1–9.
- [26] D. V. Greunen, A. J. Schutte, and M. Kleingeld, "Energy efficiency through variable speed drive control on a cascading mine cooling system," in *Proc. Int. Conf. 11th Ind. Commercial Energy*, Aug. 2014, pp. 1–6.
- [27] H. G. Brand, J. C. Vosloo, and E. H. Mathews, "Automated energy efficiency project identification in the gold mining industry," in *Proc. Int. Conf. Ind. Commercial Energy (ICUE)*, Aug. 2015, pp. 17–22.
- [28] G. E. du Plessis, E. H. Mathews, and J. C. Vosloo, "A variable water flow energy efficiency strategy for mine cooling systems," in *Proc. 10th Ind. Commercial Energy Conf.*, Aug. 2013, pp. 1–8.
- [29] B. Parkhideh, H. Mirzaee, and S. Bhattacharya, "Supplementary energy storage and hybrid front-end converters for high-power mobile mining equipment," *IEEE Trans. Ind. Appl.*, vol. 49, no. 4, pp. 1863–1872, Jul. 2013.
- [30] O. J. Abdel-Baqi, M. G. Onsager, and P. J. Miller, "The effect of available short-circuit capacity and trail cable length on substation voltage amplification in surface excavation industry," *IEEE Trans. Ind. Appl.*, vol. 52, no. 4, pp. 3518–3526, Jul./Aug. 2016.
- [31] L. Morán, C. A. Albistur, and R. Burgos, "Multimega VAR passive filters for mining applications: Practical limitations and technical considerations," *IEEE Trans. Ind. Appl.*, vol. 52, no. 6, pp. 5310–5317, Nov./Dec. 2016.
- [32] D. B. Durocher and R. Putnam, "Mining industry process upgrades to reduce energy intensity while improving end product quality," in *Proc. Workshop Power Electron. Power Qual. Appl. (PEPQA)*, Jul. 2013, pp. 1–7.
- [33] A. G. Castro, A. Moreno-Munoz, J. Garrido, S. K. Rönnberg, E. J. Palacios-Garcia, and T. Morales, "Supraharmonics reduction in NPC inverter with random PWM," in *Proc. IEEE 26th Int. Symp. Ind. Electron. (ISIE)*, Jun. 2017, pp. 1792–1797.
- [34] F. Zare, "A novel harmonic elimination method for a three-phase diode rectifier with controlled DC link current," in *Proc. 16th Int. Power Electron. Motion Control Conf. Expo.*, Sep. 2014, pp. 985–989.
- [35] O. Abdel-baqi, A. Nasiri, and P. Miller, "Dynamic performance improvement and peak power limiting using ultracapacitor storage system for hydraulic mining shovels," *IEEE Trans. Ind. Electron.*, vol. 62, no. 5, pp. 3173–3181, May 2015.
- [36] H. Mirzaee, R. Beddingfield, S. Bhattacharya, and B. Parkhideh, "Performance investigation of hybrid converter systems for mobile mining applications," in *Proc. IEEE Energy Convers. Congr. Expo.*, Sep. 2013, pp. 825–831.
- [37] Y. Wang, J. Chen, J. Liu, K. Liu, Y. Zhang, J. Wu, H. Zeng, and Z.-L. Guan, "Research and implementation of key technology of braking energy recovery system for off-highway dump truck," in *Proc. 43rd Annu. Conf. IEEE Ind. Electron. Soc.*, Oct./Nov. 2017, pp. 3912–3917.
- [38] Y. Feng, Z. Dong, J. Yang, and R. Cheng, "Performance modeling and cost-benefit analysis of hybrid electric mining trucks," in *Proc. 12th IEEE/ASME Int. Conf. Mechatronic Embedded Syst. Appl. (MESA)*, Aug. 2016, pp. 1–6.
- [39] J. Mazumdar, "All electric operation of ultraclass mining haul trucks," in *Proc. IEEE Ind. Appl. Soc. Annu. Meeting*, Oct. 2013, pp. 1–5.
- [40] J. V. Cruzat and M. A. Valenzuela, "Modeling and evaluation of benefits of trolley assist system for mining trucks," *IEEE Trans. Ind. Appl.*, vol. 54, no. 4, pp. 3971–3981, Jul./Aug. 2018.
- [41] A.-S. A. Luiz and B. de Jesus Cardoso Filho, "A new design of selective harmonic elimination for adjustable speed operation of AC motors in mining industry," in *Proc. IEEE Appl. Power Electron. Conf. Expo. (APEC)*, Mar. 2017, pp. 607–614.
- [42] T. M. Parreiras, J. C. G. Justino, A. V. Rocha, and B. D. J. C. Filho, "True unit power factor active front end for high-capacity belt-conveyor systems," *IEEE Trans. Ind. Appl.*, vol. 52, no. 3, pp. 2737–2746, May/Jun. 2016.
- [43] A. A. Luiz and B. de Jesus Cardoso Filho, "Improving power quality in mining industries with a three-level active front end," in *Proc. IEEE Ind. Appl. Soc. Annu. Meeting*, Oct. 2015, pp. 1–9.
- [44] M. G. Jahromi, G. Mirzaeva, and S. D. Mitchell, "Design and control of a high-power low-loss DC–DC converter for mining applications," *IEEE Trans. Ind. Appl.*, vol. 53, no. 5, pp. 5105–5114, Sep./Oct. 2017.
- [45] C. Tryggstad, N. Sharma, J. V. D. Staij, and A. Keizer. (2017). *New Reality: Electric Trucks and Their Implications on Energy Demand*. [Online]. Available: https://greendealzes.connekt.nl/wp-content/uploads/2017/09/MEI_eTruck_New_Reality_vP.pdf
- [46] (2018). *Battery Electric Truck and Bus Energy Efficiency Compared to Conventional Diesel Vehicles*. [Online]. Available: <https://www.arb.ca.gov/msprog/actruck/docs/HDBEVefficiency.pdfmsprog/actruck/docs/HDBEVefficiency.pdf>
- [47] M. Moultak, N. Lutsey, and D. Hall. (2017). *Transitioning to Zero-Emission Heavy-Duty Freight Vehicles*. [Online]. Available: https://www.theicct.org/sites/default/files/publications/Zero-emission-freight-trucks_ICCT-white-paper_26092017_vF.pdf
- [48] D. Kumar, F. Zare, and A. Ghosh, "DC microgrid technology: System architectures, AC grid interfaces, grounding schemes, power quality, communication networks, applications, and standardizations aspects," *IEEE Access*, vol. 5, pp. 12230–12256, 2017.
- [49] D. O. Koval, R. A. Bocancea, K. Yao, and M. B. Hughes, "Canadian national power quality survey: Frequency and duration of voltage sags and surges at industrial sites," *IEEE Trans. Ind. Appl.*, vol. 34, no. 5, pp. 904–910, Sep. 1998.
- [50] H. M. S. C. Herath, V. J. Gosbell, and S. Perera, "Power quality (PQ) survey reporting: Discrete disturbance limits," *IEEE Trans. Power Del.*, vol. 20, no. 2, pp. 851–858, Apr. 2005.
- [51] S. Elphick, P. Ciufo, V. Smith, and S. Perera, "Summary of the economic impacts of power quality on consumers," in *Proc. Australas. Univ. Power Eng. Conf. (AUPEC)*, Sep. 2015, pp. 1–6.
- [52] S. Elphick, P. Ciufo, G. Drury, V. Smith, S. Perera, and V. Gosbell, "Large scale proactive power-quality monitoring: An example from Australia," *IEEE Trans. Power Delivery*, vol. 32, no. 2, pp. 881–889, Apr. 2017.
- [53] *Electromagnetic Compatibility (EMC) Limits—Steady State Voltage Limits in Public Electricity Systems*, Standard 61000.3.100, 2011.
- [54] J. L. Duran-Gomez, P. N. Enjeti, and B. O. Woo, "Effect of voltage sags on adjustable-speed drives: A critical evaluation and an approach to improve performance," *IEEE Trans. Ind. Appl.*, vol. 35, no. 6, pp. 1440–1449, Nov. 1999.
- [55] H. B. Math, "Overview of power quality and power quality standards," in *Understanding Power Quality Problems: Voltage Sags and Interruptions*. Piscataway, NJ, USA: IEEE Press, 2000, p. 1.
- [56] M. H. J. Bollen, "Characterisation of voltage sags experienced by three-phase adjustable-speed drives," *IEEE Trans. Power Del.*, vol. 12, no. 4, pp. 1666–1671, Oct. 1997.
- [57] S. Z. Djokic, K. Stockman, J. V. Milanovic, J. J. M. Desmet, and R. Belmans, "Sensitivity of AC adjustable speed drives to voltage sags and short interruptions," *IEEE Trans. Power Del.*, vol. 20, no. 1, pp. 494–505, Jan. 2005.
- [58] J. V. Milanovic, M. T. Aung, and S. C. Vegunta, "The influence of induction motors on voltage sag propagation—Part I: Accounting for the change in sag characteristics," *IEEE Trans. Power Del.*, vol. 23, no. 2, pp. 1063–1071, Apr. 2008.
- [59] J. V. Milanovic, S. C. Vegunta, and M. T. Aung, "The influence of induction motors on voltage sag propagation—part II: Accounting for the change in sag performance at LV buses," *IEEE Trans. Power Del.*, vol. 23, no. 2, pp. 1072–1078, Apr. 2008.
- [60] A. von Jouanne and B. Banerjee, "Assessment of voltage unbalance," *IEEE Trans. Power Del.*, vol. 16, no. 4, pp. 782–790, Oct. 2001.
- [61] L. Morán, J. Espinoza, and R. Burgos, "Voltage regulation in mine power distribution systems: Problems and solutions," in *Proc. IEEE Ind. Appl. Soc. Annu. Meeting*, Oct. 2014, pp. 1–7.

- [62] T. Sukanth, S. Jayanthu, and A. Jayalaxmi, "Mitigation of power quality problem in underground mine using different control strategies," in *Proc. IEEE Region 10 Humanitarian Technol. Conf. (R-HTC)*, Dec. 2016, pp. 1–4.
- [63] D. I. Ivanchenko and E. V. Iakovleva, "Simulation of switching over-voltage in mine production unit," in *Proc. IEEE Conf. Russian Young Researchers Electr. Electron. Eng. (EIConRus)*, Feb. 2017, pp. 873–876.
- [64] *IEEE Recommended Practice and Requirements for Harmonic Control in Electric Power Systems*, IEEE Standard 519-2014 and IEEE Std 519-1992, 2014, pp. 1–29.
- [65] A. Symonds and M. Laylabadi, "Cycloconverter drives in mining applications: A typical industrial system is analyzed and the impact of harmonic filtering considered," *IEEE Ind. Appl. Mag.*, vol. 21, no. 6, pp. 36–46, Nov/Dec. 2015.
- [66] *Electromagnetic Compatibility (EMC) Part 2-4: Environment-Compatibility Levels in Industrial Plants for Low-Frequency Conducted Disturbances*, IEC Standard 61000-2-4, 2002.
- [67] *Electromagnetic Compatibility (EMC) Part 3-6: Limits-Assessment of Emission Limits for the Connection of Distorting Installations to MV, HV and EHV Power Systems*, IEC Standard 61000-3-6, 2008.
- [68] *IEEE Recommended Practices and Requirements for Harmonic Control in Electrical Power Systems*, IEEE Standard 519-1992, pp. 1–112, 1993.
- [69] T. S. de Souza, A.-S. A. Luiz, and M. M. Stopa, "An assessment of harmonic filter for indirect field oriented induction motor drives in mining industry," in *Proc. 12th IEEE Int. Conf. Ind. Appl. (INDUSCON)*, Nov. 2016, pp. 1–8.
- [70] A.-S. A. Luiz and M. M. Stopa, "An alternative five level NPC converter for medium voltage AC drives and technical issues," in *Proc. IEEE 13th Brazilian Power Electron. Conf. 1st Southern Power Electron. Conf. (COBEP/SPEC)*, Nov/Dec. 2015, pp. 1–6.
- [71] S. Hansen, P. Nielsen, and F. Blaabjerg, "Harmonic cancellation by mixing nonlinear single-phase and three-phase loads," *IEEE Trans. Ind. Appl.*, vol. 36, no. 1, pp. 152–159, Jan./Feb. 2000.
- [72] D. Kumar and F. Zare, "Harmonic analysis of grid connected power electronic systems in low voltage distribution networks," *IEEE Trans. Emerg. Sel. Topics Power Electron.*, vol. 4, no. 1, pp. 70–79, Mar. 2016.
- [73] A. Testa et al., "Interharmonics: Theory and modeling," *IEEE Trans. Power Del.*, vol. 22, no. 4, pp. 2335–2348, Oct. 2007.
- [74] M. B. Rifai, T. H. Ortmeyer, and W. J. McQuillan, "Evaluation of current interharmonics from ac drives," *IEEE Trans. Power Del.*, vol. 15, no. 3, pp. 1094–1098, Jul. 2000.
- [75] F. De Rosa, R. Langella, A. Sollazzo, and A. Testa, "On the interharmonic components generated by adjustable speed drives," *IEEE Trans. Power Del.*, vol. 20, no. 4, pp. 2535–2543, Oct. 2005.
- [76] H. Soltani, F. Blaabjerg, F. Zare, and P. C. Loh, "Effects of passive components on the input current interharmonics of adjustable-speed drives," *IEEE J. Emerg. Sel. Topics Power Electron.*, vol. 4, no. 1, pp. 152–161, Mar. 2016.
- [77] E. W. Gunther, "Interharmonics in power systems," in *Proc. IEEE Power Eng. Soc. Summer Meeting*, Jul. 2001, pp. 813–817.
- [78] J. Arrillaga, N. R. Watson, and S. Chen, *Power System Quality Assessment*. Hoboken, NJ, USA: Wiley, 2000.
- [79] Z. Hanzelka and A. Bien, "Power quality application guide," *Copper Develop. Assoc. IEE Endorsed Provider*, Jul. 2004.
- [80] D. Gallo, R. Langella, and A. Testa, "Light flicker prediction based on voltage spectral analysis," in *Proc. IEEE Porto Power Tech*, Sep. 2001, p. 6.
- [81] D. Gallo, C. Landi, R. Langella, and A. Testa, "IEC flickermeter response to interharmonic pollution," presented at the 11th Int. Conf. Harmon. Qual. Power, Lake Placid, NY, USA, 2004.
- [82] M. Hernes and B. Gustavsen, "Simulation of shaft vibrations due to interaction between turbine-generator train and power electronic converters at the Visund oil platform," in *Proc. Power Convers. Conf.*, Apr. 2002, pp. 1381–1386.
- [83] F. Wang and M. H. J. Bollen, "Measurement of 182 Hz interharmonics and their impact on relay operation," in *Proc. 9th Int. Conf. Harmon. Qual. Power*, Oct. 2000, pp. 55–60.
- [84] D. Basic, "Input current interharmonics of variable-speed drives due to motor current imbalance," *IEEE Trans. Power Del.*, vol. 25, no. 4, pp. 2797–2806, Oct. 2010.
- [85] H. Soltani, P. Davari, F. Zare, P. C. Loh, and F. Blaabjerg, "Characterization of input current interharmonics in adjustable speed drives," *IEEE Trans. Power Electron.*, vol. 32, no. 11, pp. 8632–8643, Nov. 2017.
- [86] *Electromagnetic compatibility (EMC)—Part 4-7: Testing and Measurement Techniques-General Guide on Harmonics and Interharmonics Measurements and Instrumentation, for Power Supply Systems and Equipment Connected Thereto*, IEC Standard 61000-4-7, 2002.
- [87] C.-I. Chen and Y.-C. Chen, "Comparative study of harmonic and inter-harmonic estimation methods for stationary and time-varying signals," *IEEE Trans. Ind. Electron.*, vol. 61, no. 1, pp. 397–404, Jan. 2014.
- [88] C.-I. Chen and G. W. Chang, "An efficient Prony-based solution procedure for tracking of power system voltage variations," *IEEE Trans. Ind. Electron.*, vol. 60, no. 7, pp. 2681–2688, Jul. 2013.
- [89] I. Y.-H. Gu and M. H. J. Bollen, "Estimating interharmonics by using sliding-window ESPRIT," *IEEE Trans. Power Del.*, vol. 23, no. 1, pp. 13–23, Jan. 2008.
- [90] M. Karimi-Ghartemani and M. R. Iravani, "Measurement of harmonics/inter-harmonics of time-varying frequencies," *IEEE Trans. Power Del.*, vol. 20, no. 1, pp. 23–31, Jan. 2005.
- [91] I. Sadinezhad and V. G. Agelidis, "Frequency adaptive least-squares-Kalman technique for real-time voltage envelope and flicker estimation," *IEEE Trans. Ind. Electron.*, vol. 59, no. 8, pp. 3330–3341, Aug. 2012.
- [92] H. Soltani, P. C. Loh, F. Blaabjerg, and F. Zare, "Interharmonic analysis and mitigation in adjustable speed drives," in *Proc. 40th Annu. Conf. IEEE Ind. Electron. Soc.*, Oct./Nov. 2014, pp. 1556–1561.
- [93] E. J. Delaney and R. E. Morrison, "Minimisation of interharmonic currents from a current source AC drive by means of a selective DC side active filter," *IEEE Trans. Power Del.*, vol. 10, no. 3, pp. 1584–1590, Jul. 1995.
- [94] H. Soltani, P. C. Loh, F. Blaabjerg, and F. Zare, "Interharmonic mitigation of adjustable speed drives using an active DC-link capacitor," in *Proc. 9th Int. Conf. Power Electron. ECCE Asia (ICPE-ECCE Asia)*, Jun. 2015, pp. 2018–2024.
- [95] H. Soltani, P. C. Loh, F. Blaabjerg, and F. Zare, "Sources and mitigation of interharmonics in back-to-back controllable drives," in *Proc. 16th Eur. Conf. Power Electron. Appl.*, Aug. 2014, pp. 1–9.
- [96] H. Soltani, P. Davari, F. Blaabjerg, and F. Zare, "Performance evaluation of electronic inductor based adjustable speed drives with respect to line current interharmonics," in *Proc. IEEE Appl. Power Electron. Conf. Expo. (APEC)*, Mar. 2017, pp. 3171–3178.
- [97] H. Soltani, P. Davari, F. Zare, and F. Blaabjerg, "Effects of modulation techniques on the input current interharmonics of adjustable speed drives," *IEEE Trans. Ind. Electron.*, vol. 65, no. 1, pp. 167–178, Jan. 2018.
- [98] M. Bollen, "Future work on harmonics—Some expert opinions part I—Wind and solar power," in *Proc. 16th Int. Conf. Harmon. Qual. Power (ICHQP)*, May 2014, pp. 904–908.
- [99] J. Meyer, "Future work on harmonics—Some expert opinions part II—Supraharmonics, standards and measurements," in *Proc. IEEE 16th Int. Conf. Harmon. Qual. Power (ICHQP)*, May 2014, pp. 909–913.
- [100] A. Gil-de-Castro, S. K. Rönnerberg, and M. H. J. Bollen, "A study about harmonic interaction between devices," in *Proc. 16th Int. Conf. Harmon. Qual. Power (ICHQP)*, May 2014, pp. 728–732.
- [101] M. Klatt, J. Meyer, P. Schegner, R. Wolf, and B. Wittenberg, "Filter for the measurement of supraharmonics in public low voltage networks," in *Proc. IEEE Int. Symp. Electromagn. Compat. (EMC)*, Aug. 2015, pp. 108–113.
- [102] T. Rehman, J. Yaghoobi, and F. Zare, "Harmonic issues in future grids with grid connected solar inverters: 0-9 kHz," presented at Australas. Univ. Power Eng. Conf. (AUPEC), Auckland, New Zealand, vol. 1, Nov. 2018.
- [103] J. Yaghoobi, F. Zare, T. Rehman, and H. Rathnayake, "Analysis of high frequency harmonics in distribution networks: 9–150 kHz," in *Proc. ICIT*, Melbourne, VIC, Australia, Feb. 2019, p. 6.
- [104] D. Semenov, B. Tian, S. Li, and G. Mirzaeva, "Advanced fault-tolerant current control of five-phase PMSM for mining applications," in *Proc. IEEE Ind. Appl. Soc. Annu. Meeting*, Oct. 2016, pp. 1–7.
- [105] M. H. J. Bollen and L. D. Zhang, "Analysis of voltage tolerance of AC adjustable-speed drives for three-phase balanced and unbalanced sags," *IEEE Trans. Ind. Appl.*, vol. 36, no. 3, pp. 904–910, May 2000.
- [106] J. Pedra, F. Corcoles, and F. J. Suelves, "Effects of balanced and unbalanced voltage sags on VSI-fed adjustable-speed drives," *IEEE Trans. Power Del.*, vol. 20, no. 1, pp. 224–233, Jan. 2005.
- [107] M. H. J. Bollen and R. A. A. de Graaff, "Behavior of AC and DC drives during voltage sags with phase-angle jump and three-phase unbalance," in *Proc. IEEE Power Eng. Soc.*, vol. 2, Jan./Feb. 1999, pp. 1225–1230.

- [108] K. Lee, T. M. Jahns, T. A. Lipo, G. Venkataramanan, and W. E. Berkopec, "Impact of input voltage sag and unbalance on DC-link inductor and capacitor stress in adjustable-speed drives," *IEEE Trans. Ind. Appl.*, vol. 44, no. 6, pp. 1825–1833, Nov./Dec. 2008.
- [109] K. Lee, G. Venkataramanan, and T. M. Jahns, "Modeling effects of voltage unbalances in industrial distribution systems with adjustable-speed drives," *IEEE Trans. Ind. Appl.*, vol. 44, no. 5, pp. 1322–1332, Sep./Oct. 2008.
- [110] S.-G. Jeong and J.-Y. Choi, "Line current characteristics of three-phase uncontrolled rectifiers under line voltage unbalance condition," *IEEE Trans. Power Electron.*, vol. 17, no. 6, pp. 935–945, Nov. 2002.
- [111] K. Lee, G. Venkataramanan, and T. M. Jahns, "Source current harmonic analysis of adjustable speed drives under input voltage unbalance and sag conditions," *IEEE Trans. Power Del.*, vol. 21, no. 2, pp. 567–576, Apr. 2006.
- [112] K. Lee, T. M. Jahns, G. Venkataramanan, and W. E. Berkopec, "DC-bus electrolytic capacitor stress in adjustable-speed drives under input voltage unbalance and sag conditions," *IEEE Trans. Ind. Appl.*, vol. 43, no. 2, pp. 495–504, Mar./Apr. 2007.
- [113] H. Wang, P. Davari, D. Kumar, F. Zare, and F. Blaabjerg, "The impact of grid unbalances on the reliability of DC-link capacitors in a motor drive," in *Proc. IEEE Energy Convers. Congr. Expo. (ECCE)*, Oct. 2017, pp. 4345–4350.
- [114] *Electrolytic Capacitor Catalog*, Evox Rifa Group, Kalmar, Sweden, 2003, vol. 14.
- [115] K. Lee, T. M. Jahns, W. E. Berkopec, and T. A. Lipo, "Closed-form analysis of adjustable-speed drive performance under input-voltage unbalance and sag conditions," *IEEE Trans. Ind. Appl.*, vol. 42, no. 3, pp. 733–741, May 2006.
- [116] K. Lee, T. Jahns, D. W. Novotny, T. A. Lipo, W. E. Berkopec, and V. Blasko, "Impact of inductor placement on the performance of adjustable-speed drives under input voltage unbalance and sag conditions," *IEEE Trans. Ind. Appl.*, vol. 42, no. 5, pp. 1230–1240, Sep./Oct. 2006.
- [117] M. Petronijevic, B. Veselic, N. Mitrovic, V. Kostic, and B. Jęftenic, "Comparative study of unsymmetrical voltage sag effects on adjustable speed induction motor drives," *IET Electric Power Appl.*, vol. 5, no. 5, pp. 432–442, May 2011.
- [118] D. D. Shipp and W. S. Vilcheck, "Power quality and line considerations for variable speed AC drives," *IEEE Trans. Ind. Appl.*, vol. 32, no. 2, pp. 403–410, Mar. 1996.
- [119] R. Ghandehari and A. Shoulaie, "Evaluating voltage notch problems arising from AC/DC converter operation," *IEEE Trans. Power Electron.*, vol. 24, no. 9, pp. 2111–2119, Sep. 2009.
- [120] L. Tang, M. McGranaghan, R. Ferraro, S. Morganson, and B. Hunt, "Voltage notching interaction caused by large adjustable speed drives on distribution systems with low short circuit capacities," *IEEE Trans. Power Del.*, vol. 11, no. 3, pp. 1444–1453, Jul. 1996.
- [121] A. H. Hoevenaars, I. C. Evans, and B. Desai, "Preventing AC drive failures due to commutation notches on a drilling rig," *IEEE Trans. Ind. Appl.*, vol. 49, no. 3, pp. 1215–1220, May/Jun. 2013.
- [122] F. Zare and D. Kumar, "Harmonics analysis of industrial and commercial distribution networks with high penetration of power electronics converters," in *Proc. Australas. Univ. Power Eng. Conf. (AUPEC)*, Sep. 2016, pp. 1–6.



AHMAD ABDULLAH was born in Rawalpindi, Punjab, Pakistan, in 1991. He received the B.Sc. degree in electrical engineering from the University of Engineering and Technology, Lahore, in 2013, and the M.Phil. degree from the University of Queensland, under the supervision of Dr. F. Zare.

From 2013 to 2017, he was an Electrical Engineer with Fatima Fertilizer Company Limited, Sadiqabad, Pakistan. He is currently a Testing and Assessment Officer with the Safety in mining, testing and research station (Simtars), Department of Natural Resources, Mines and Energy, Queensland. His current research interests include power electronics, power system distribution, power system analysis, and hazardous area electrical equipment. Mr. Abdullah is a member of the Institution of Engineers Australia.



DINESH KUMAR (S'08–M'12) received the M.Tech. degree in power system engineering from IIT, Roorkee, India, in 2004, and the Ph.D. degree in power electronics from the University of Nottingham, U.K., in 2010. From 2004 to 2005, he served as a Lecturer with the Electrical Engineering Department, National Institute of Technology, Kurukshetra, India. In 2006, he joined Technical University Chemnitz, Germany, as a Research Fellow. From 2006 to

2010, he investigated and developed matrix converter based multidrive system for aerospace applications. Since 2011, he has been with the Danfoss Drives A/S, Denmark, where he is involved in many research and industrial projects. His current research interests include motor drive, harmonic analysis and mitigation techniques, power quality, and electromagnetic interference in power electronics. He is the Editor-in-Chief of the *International Journal of Power Electronics* and the Associate Editor of the *IEEE TRANSACTION ON INDUSTRY APPLICATIONS* and *IEEE ACCESS* Journal.



FIRUZ ZARE (S'98–M'01–SM'06) received the Ph.D. degree in power electronics from the Queensland University of Technology, Australia, in 2002. He has spent several years in industry as a team leader involved in power electronics and power quality projects. He is currently an Academic Staff with The University of Queensland, Australia and a Task Force Leader of Active Infeed Converters within Working Group one at the IEC standardization TC77A. He has published over

220 journal and conference papers and technical reports in power electronics. His current research interests include power electronics topology, control and applications; power quality and regulations; and pulsed power applications. Prof. Zare has received several awards, such as an Australian Future Fellowship, Symposium Fellowship from the Australian Academy of Technological Science, the Early Career Academic Excellence Research Award, and the John Madsen Medal from Engineers Australia. He is an Editor-in-Chief of the *International Journal of Power Electronics* and the Associate Editor of *IEEE ACCESS* journal and the *IEEE JOURNAL OF EMERGING AND SELECTED TOPICS IN POWER ELECTRONICS*.



HAMID SOLTANI (S'14–M'16) received the B.Sc. and M.Sc. degrees in electrical engineering from the University of Mazandaran (Noushivani), Babol, Iran, in 2005 and 2008, respectively, and the Ph.D. degree in power electronics from Aalborg University, Aalborg, Denmark, in 2016. From 2009 to 2013, he was with the Department of Electrical and Computer Engineering, Golestan University, Gorgan, Iran, as a Lecturer. He was also a Postdoctoral Researcher with the Department of Energy Technology, Aalborg University, from 2016 to 2017. He is currently with the Department of Converter Control, Vestas Wind Systems A/S, Aarhus, Denmark. His current research interests include wind energies, power quality, and power electronics topologies and control.



JALIL YAGHOOBI (M'11) was born in Zahedan, Iran, in 1985. He received the B.Sc. and M.Sc. degrees in electrical engineering from the Sharif University of Technology (SUT), Tehran, Iran, in 2008 and 2011, respectively, and the Ph.D. degree in power engineering from the University of Queensland (UQ), Brisbane, QLD, Australia, in 2016.

Since 2016, he has been a Postdoctoral Research Fellow with the School of Information Technology and Electrical Engineering (ITEE), The University of Queensland (UQ), St. Lucia. He is the author of more than 15 articles. His current research interests include power quality and high-frequency harmonics, power electronics, renewable energy integration in power systems, and energy efficiency.

He has also been an active member of the IEEE Power and Energy Society, since 2012.